ISSN 0024-4902, Lithology and Mineral Resources, 2008, Vol. 43, No. 4, pp. 354–379. © Pleiades Publishing, Inc., 2008.
Original Russian Text © Yu.O. Gavrilov, E.V. Shchepetova, M.A. Rogov, E.A. Shcherbinina, 2008, published in Litologiya i Poleznye Iskopaemye, 2008, No. 4, pp. 396–424.

Sedimentology, Geochemistry, and Biota of Volgian Carbonaceous Sequences in the Northern Part of the Central Russian Sea (Kostroma Region)

Yu. O. Gavrilov, E. V. Shchepetova, M. A. Rogov, and E. A. Shcherbinina

Geological Institute, Russian Academy of Sciences, Pyzhevskii per. 7, Moscow, 119017 Russia
e-mail: gavrilov@ginras.ru, shchepetova@ginras.ru

Received January 28, 2008

Abstract—Lithological, geochemical, stratigraphic, and paleoecological features of carbonaceous sediments in the Late Jurassic Volgian Basin of the East European Platform (Kostroma region) are considered. The shale-bearing sequence studied is characterized by greater sedimentological completeness as compared with its stratotype sections in the Middle Volga region (Gorodishche, Kashpir). Stratigraphic position and stratigraphy of the shale-bearing sequence, as well as the distribution of biota in different sedimentation settings, are specified. It is shown that Volgian sediments show a distinct cyclic structure. The lower and upper elements of cyclites consist of high-carbonaceous shales and clayey–calcareous sediments, respectively, separated by transitional varieties. Bioturbation structures in different rocks are discussed. Microcomponent composition and pyrolytic parameters of organic matter, as well as distribution of chemical elements in the lithologically variable sediments are analyzed. Possible reasons responsible for the appearance of cyclicity and accumulation of organic-rich sediments are discussed.

DOI: 10.1134/S002449020804007X

The second half of the Late Jurassic Period was characterized by the development of conditions favorable for the accumulation of high-carbonaceous (frequently, oil-generating) sediments in different regions of the Northern Hemisphere (West Europe, Russian Plate, Barents Sea, West Siberia, and others). In the East European Platform, organic-rich sediments of the Volgian Stage (oil shales) are developed over a spacious area. Researchers have proposed different concepts for the accumulation of high-carbonaceous sediments. However, formation mechanisms of such sediments remain unclear so far. Development of their genetic models requires data on sections from different parts of the spacious Volgian Basin, which would make it possible to understand general regularities in its evolution and determine the influence of local factors on sedimentation processes. Data on the typical shale-bearing sections with the most complete record of their sedimentation history are also essential.

The best studied Gorodishche and Kashpir stratotype sections of the Volgian Stage in the Middle Volga region represent the relatively condensed successions with numerous indications of syn- and postsedimentary erosion. This process promoted the concentration of coarse fractions at some levels, i.e., in the formation of condensed units (Baraboshkin et al., 2002). In case of exhumation of the relatively compact sediments to the basin bottom, they were subjected frequently (often intensely) reworked by burrowing organisms, resulting in the formation of softground-type surface (Bromley, 1996). These and some other phenomena were responsible for the fragmentary record of the shale-bearing sequence formation in sections of the Volga region.

Such disadvantages of the sedimentation record are significantly less manifested in the examined section near the Ivkino Settlement located on the right bank of the Unzha River (left tributary of the Volga River, Kostroma region) in the area known as the Manturov group of Volgian oil shale deposits (Dobryanskii, 1947; Yavkhuta, 1973; and others) (Fig. 1).

In addition to the relative sedimentary completeness, the Ivkino shale-bearing section is also interesting from the standpoint of sedimentation settings in the northern (least studied) part of the Volgian Basin. In this work, we present a detailed characteristic of the shale-bearing sequence with the consideration of different sedimentological and geochemical features, which are crucial for understanding sedimentation settings of the Volgian carbonaceous sediments.

When studying the shale-bearing sequence and the underlying and overlying sediments, we paid particular attention to the initial structure of sediments, degree of biogenic reworking, character of bioturbation, grain-size distribution, mineral composition, petrographic and pyrolytic parameters of organic matter (OM), and distribution of different chemical elements in the heterogeneous laminated sequence.

It should be noted that the shale-bearing sequence is overlain by Cretaceous and Quaternary sediments with

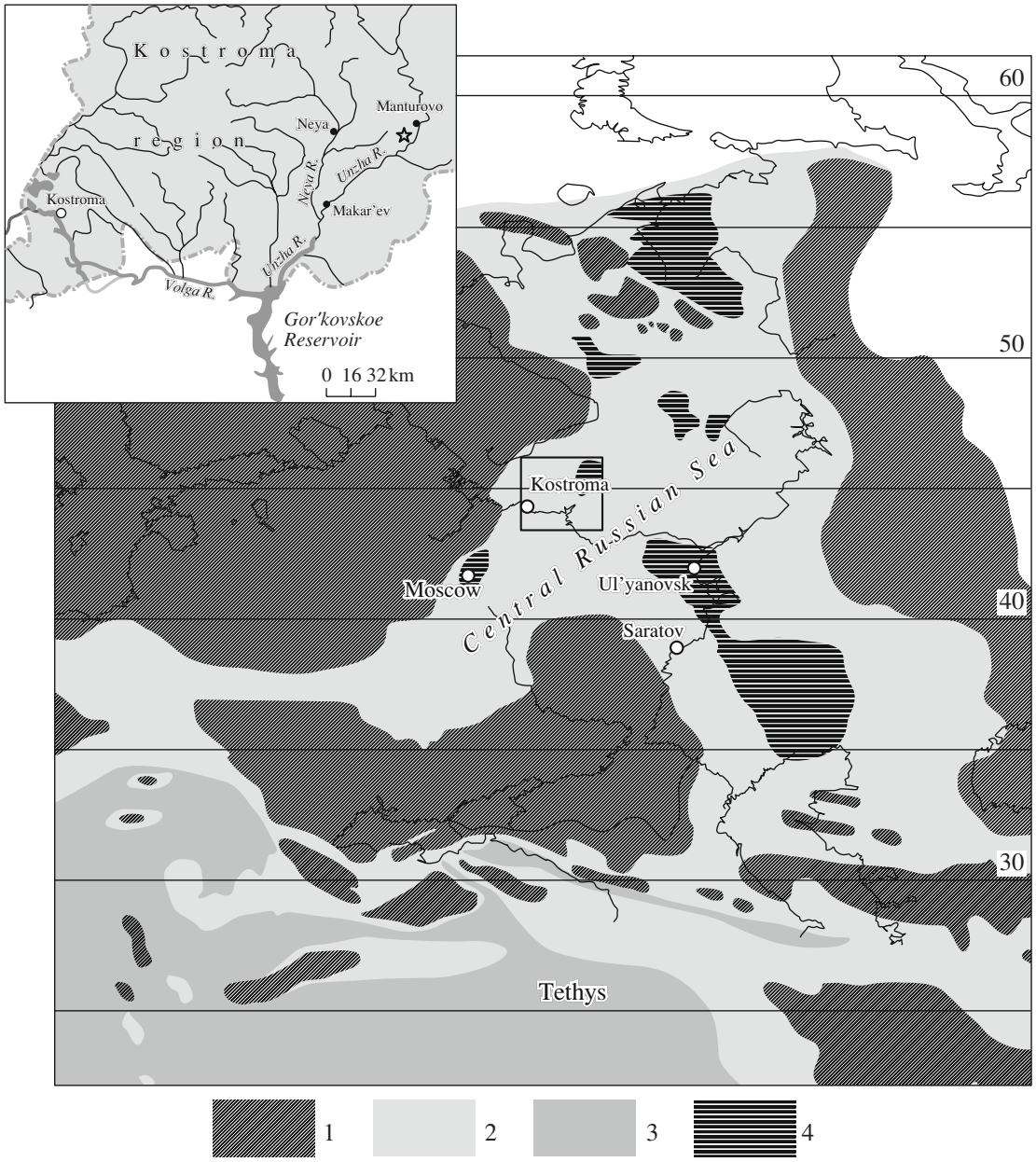

Fig. 1. Schematic paleogeographic map of the East European Platform for the Volgian Age (sea and land distribution, after (Thierry, 2000); areas of shale-bearing sequence development, after (*Prognoz goryuchikh...*, 1974; Lyyurov, 1996; and others). (1) Land; (2) epicontinental seas; (3) Tethys Ocean; (4) areas of shale-bearing sequence development. Asterisk in the inset shows location of the Ivkino section.

the total thickness of 150 m. Intensity of postsedimentary transformations of the shale-bearing sediments corresponds to early catagenesis. Consequently, the present-day geochemical parameters reflect largely their state at sedimentary and diagenetic stages.

The mineral composition of rocks was determined by the X-ray diffraction method in the Laboratory of Physical Methods for the Study of Rock-Forming Minerals (GIN). Pyrolytic parameters were measured using a Rock-Eval II equipment at the Institute of Geology and Development of Fuel Minerals. Concentrations of C_{org}, CO_2, Fe, Mn, Ti, P, and S were determined by chemical methods, while concentrations of other elements were measured by the emission spectral method (spectrometer PGS-1) in the Laboratory of Physical Methods for the Study of Rock-Forming Minerals (GIN).

Particular attention was paid to specification of the stratigraphic position of the examined sequence and response of the biota to sharp fluctuations of paleoecological settings during the accumulation of alternating high- and low-carbonaceous sediments. The obtained

data are important for the more reliable correlation of sections in the spacious East European Platform and the elucidation of relationships between the Volgian shale-bearing sequence and carbonaceous sediments in other regions of the Northern Hemisphere. Ammonites and nannofossils were the main objects in these studies, although other fossil remains were also taken into consideration.

GENERAL CHARACTERISTIC AND STRATIGRAPHIC POSITION OF THE SHALE-BEARING SEQUENCE

The present-day spacious fields of Volgian high-carbonaceous sediments make up the Volga–Pechora shale-bearing province (Fig. 1) in the eastern Russian Plate (Yavkhuta, 1973). They constitute a sequence with well-developed bedding related to the alternation of beds (thickness from *n* dm to ~1 m or more) of dark brown high-carbonaceous shales and notably lighter (mainly gray) clayey–calcareous sediments. The thickness of sequence varies from a few meters in the Russian Plate to several tens of meters in the southern and northeastern parts. The shales extend laterally over significant distances (more than 10*n* km) only in rare cases and their amount in the sequence is variable. The shale-bearing sequence is frequently replaced laterally by condensed sections composed of phosphorites, carbonate and siliceous coquinas, and glauconitic sandstones.

Although shale-bearing sediments are known in the Kostroma and northern regions for more than a century (Krotov, 1879; Ivanov, 1909; Rozanov, 1913; Dobryanskii, 1947, Gerasimov et al., 1962; Yavkhuta, 1973), data on the structure of their particular sections are lacking. Territory characterized by the preservation of these sediments form erosion is bounded by the sublatitudinal line extending from Manturovo to Neya in the north and to the Unzha Settlement in the south. They occur at depths of 0 to 50 m and their thickness increases gradually from 0.9 m in the Unzha Settlement area to ~8 m near Manturovo; i.e., one can see transition from the condensed section (Gerasimov et al., 1962) to the more or less complete section.

Olfer'ev (1986) identified Volgian sediments (oil shales) of the Kostroma region into the Kostroma Formation and proposed to consider sections outcropping at the right bank of the Unzha River as its stratotypes. The Ivkino section (58°14′36″ N, 44°39′29″ E) is one of them.

Based on lithology, the Ivkino section is divided into three sequences: the lower Kimmeridgian sequence of calcareous clays (apparent thickness approximately 1.2 m), the middle Volgian shale-bearing sequence (~6 m thick) subdivided into three members, and the overlying sandstone–siltstone sequences (Fig. 2).

Results of the Study of Ammonites and Other Macrofaunal Fossils

Already at the beginning of stratigraphic studies in the early 20th century, it was established that the shale-bearing sequence correlates with the *Dorsoplanites panderi* ammonite zone of the middle Volgian Substage (initially, *Perisphinctes panderi* Zone of the Volgian Stage). Identification of this zone was followed by attempts to subdivide it into smaller units (Rozanov, 1919; Ilovaiskii and Florenskii, 1941). Mikhailov (1962): the lower *Pavlovia pavlovi* Subzone and the upper *Dorsoplanites panderi* Subzone, which was later renamed as *Zaraiskites zarajskensis* Subzone (Gerasimov and Mikhailov, 1966).

Based on the *Zaraiskites* phyletic lineage (from the base to top: *quenstedti, scythicus, regularis, zarajskensis*), Kutek (1994) subdivided the *Scythicus* Zone, an analogue of the *Panderi* Zone (Poland), into two subzones and four faunal horizons. In the Russian Plate, this stratigraphic interval can also be subdivided into two subzones (based on the *Zaraiskites* ammonite species): *Scythicus* and *Zarajskensis*. Recently, *Zaraiskites regularis* was found in the Russian Plate (Rogov, 2004). Subsequently, all the four faunal horizons defined by Kutek in Poland were established in the Gorodishche section of the Middle Volga region (Rogov, 2005). The species *Zaraiskites regularis* is subdivided in two chronological subspecies that characterize successive faunal horizons (Pimenov et al., 2005).

It was noted long ago that the boreal (cold-resistant) ammonite species of the genera *Pavlovia* and *Dorsoplanites* prevail in northern areas of the Russian Plate, while assemblages from its central areas are dominated by the Subboreal (relatively more thermophilic) *Zaraiskites* forms (Rozanov, 1913).

Until recently, stratigraphy of the Volgian sediments was not virtually studied in the Kostroma region. Among recent publications, one can note a find of the ammonite species *Pavlovia pavlovi* in the Ivkino section (Mitta and Starodubtseva, 1998), a species characteristic of the *Panderi* Zone in the Russian Plate. This find confirmed the previously established age of the shale-bearing sequence.

The lower part of the Ivkino section contains the lower Kimmeridgian ammonite species *Amoebites* sp. and *Rasenia* sp. characteristic of the *Cymodoce* Zone (Fig. 2), which occur as both deformed clayey casts of shells and phosphatized body chambers.

The upper Kimmeridgian and lower Volgian sediments are absent in the section. The boundary between stages is distinctly indicated by a regional thin interbed of phosphoritic conglomerate with reworked Kimmeridgian ammonites. The next phosphorite interbed, which occurs approximately 0.17 m above the previous one, is likely of the middle Volgian age because it contains rare *Dorsoplanites* cf. *dorsoplanus* (Fig. 2).

Based on numerous finds of ammonite genera *Pavlovia, Dorsoplanites*, and *Zaraiskites*, the shale-bearing

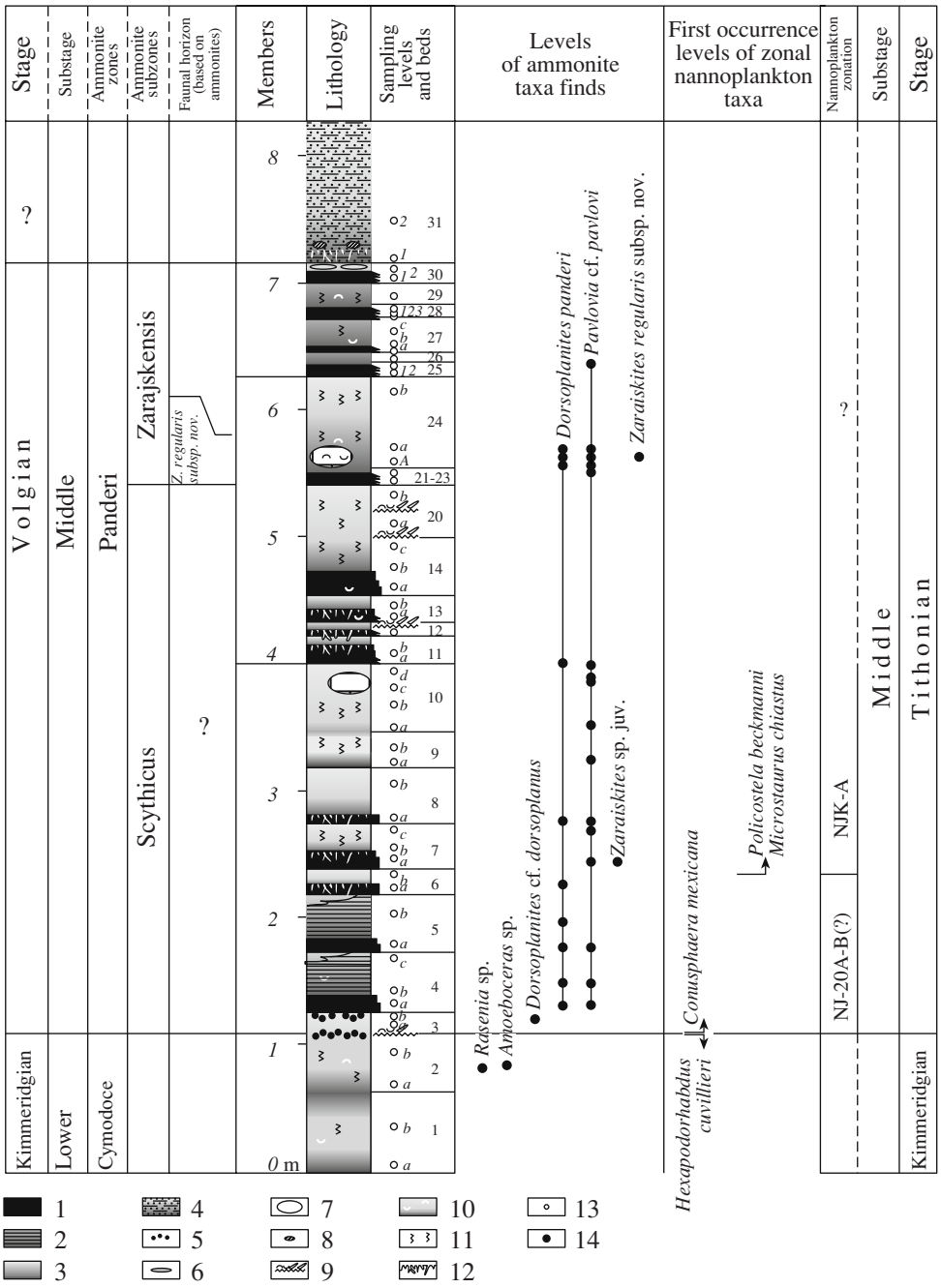

Fig. 2. Schematic stratigraphy of the Ivkino section and distribution of guide ammonite and nannoplankton species. (1) Carbonaceous shales; (2) laminated calcareous–clayey rocks; (3) massive calcareous–clayey rocks; (4) clayey–sandy siltstones; (5) phosphorite pebbles and nodules; (6) phosphate concretions; (7) calcareous concretions; (8) pyrite nodules; (9) erosion and sediment condensation surfaces; (10) fossils; (11) bioturbation; (12) "softground" with fucoids confined to levels of decelerated sedimentation or nondeposition, after (Bromley, 1996); (13) sampling sites; (14) ammonite finds.

sequence is reliably correlated with the *Panderi* Zone of the middle Volgian Substage.

Ammonite shells in the Ivkino section are strongly deformed and unidentifiable in some cases. Nevertheless, it is evident that finds of the boreal ammonites *Pavlovia pavlovi* and *Dorsoplanites* are most common (>98%) and the former species is particularly abundant. In the lower part of the section, *P. pavlovi* (Figs. 3b, 3c) specimens are usually small, which is generally characteristic of the lower part of the *Panderi* Zone in the Russian Plate (Fig. 3a). Only Bed 24 contains the relatively large specimens (Fig. 3e). In small *Dorsoplanites* specimens, their generic features are often poorly developed, which makes them almost indistinguishable from

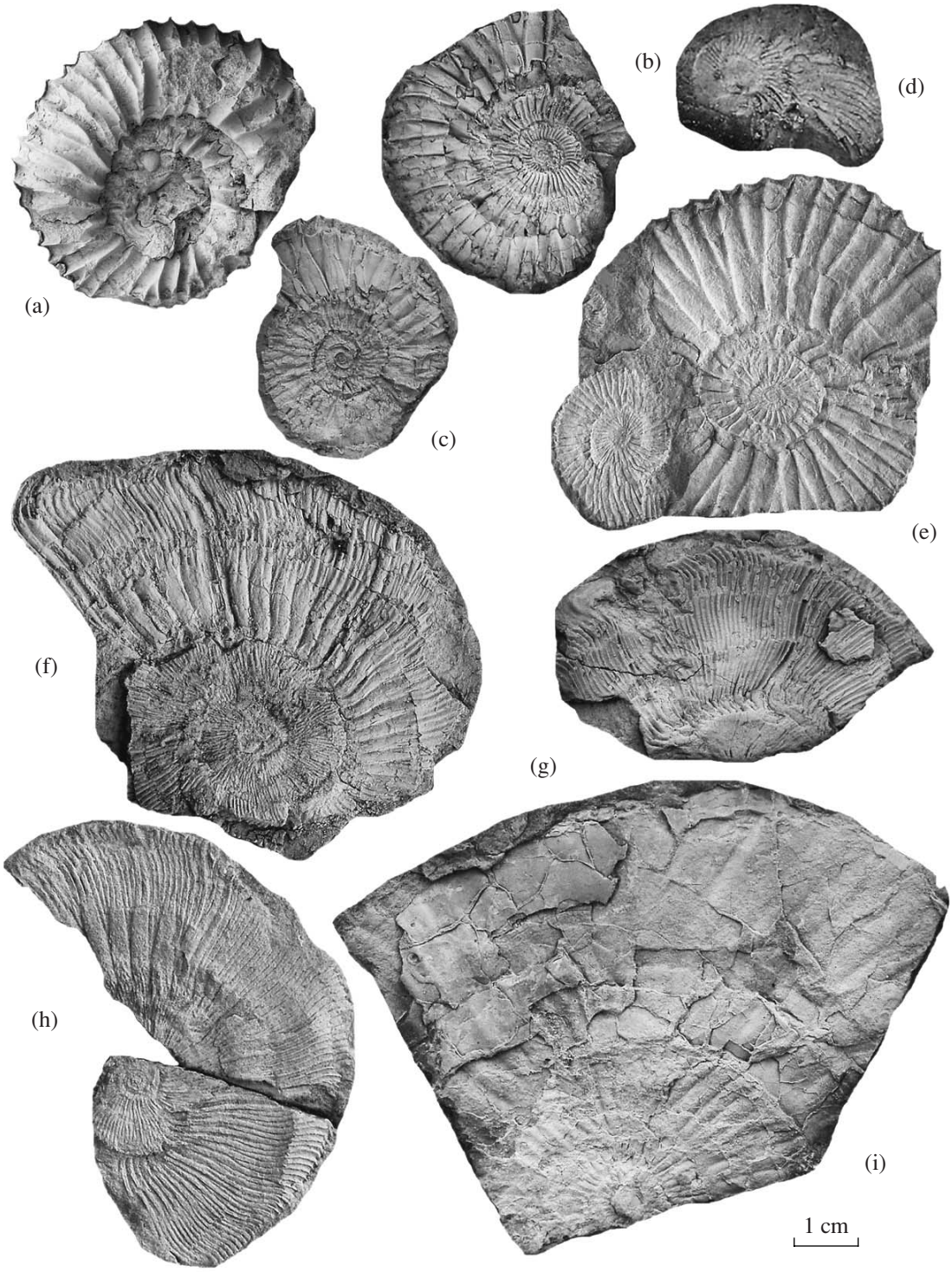

Fig. 3. Ammonites from the *Panderi* Zone of the middle Volgian Substage. (a–c, e) *Pavlovia pavlovi* (Mikhalski): (a) Specimen MK2341, Khanskaya Gora section, Berdyanka River, *Scythites* Subzone, Bed C7, (b) Specimen MK2321, Ivkino section, *Scythites*(?) Subzone, Bed 7, (c) Specimen MK2320, Ivkino section, *Scythites*(?) Subzone, Bed 8, (e) Specimen MK2466, *Zarajskensis* Subzone, *regularis* subsp. nov. faunal horizon, Ivkino section, Bed 24 (collection by E.K. Iosifova); (d) *Zaraiskites* sp. juv. (cf. *scythicus* (Vischn.)), Specimen MK2307-2, *Scythicus* Subzone, Ivkino section, Bed 7; (f, h) *Zaraiskites regularis* subsp. nov., *Zarajskensis* Subzone, *regularis* subsp. nov. faunal horizon: (f) Specimen MK1250, Kashpir section, Bed 2/10, (h) Specimen MK2467, Ivkino section, Bed 24 (collection by E.K. Iosifova); (g) *Zaraiskites* sp., Specimen 66J1, *Zarajskensis* Subzone, *regularis* subsp. nov. (?) faunal horizon, Sysola River, Bed Yb; (i) *Dorsoplanites* cf. *panderi* (Eichw.), Specimen MK2464, *Zarajskensis* Subzone, *regularis* subsp. nov. faunal horizon, Ivkino section, Bed 24 (collection by E.K. Iosifova). Depository of the Geological Institute (specimens from the collection by M.A. Rogov unless otherwise stated. Scale bar 1 cm (magn. 1.5 in 3d).

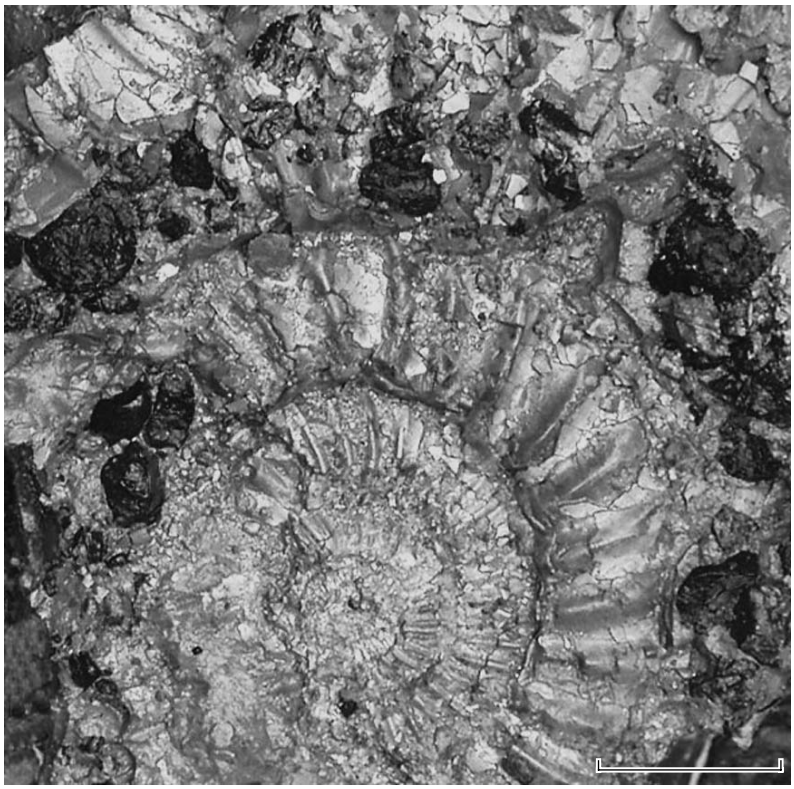

Fig. 4. Fragment of the prepared surface of phosphorite bed (roof of Bed 3) with inclusions of phosphorite nodules (black) and ammonite casts *Dorsoplanites* cf. *dorsoplanus* (Vischn.), *Panderi* Zone of the middle Volgian Substage. Photograph by M.A. Rogov. Scale bar 5 cm.

Pavlovia representatives of the similar size. Therefore, their share in the ammonite assemblage is unclear so far. *Dorsoplanites* cf. *dorsoplanus* is found at the base of Volgian sediments (Fig. 4). *D.* cf. *panderi* (Fig. 3i) occurs slightly higher in the section.

In northern areas of the Russian Plate, *Zaraiskites* suitable for the subdivision of the *Panderi* Zone into faunal horizons are rare. They are unknown in the lower part of this zone because of paleobiogeographic reasons (Rogov, 2005). Sections of the Pechora (Repin et al., 2006) and Sysola river basins contain only *Z. regularis.* In the Ivkino section, specimens of *Zaraiskites* are found at two stratigraphic levels: the lower part of the section (Bed 7) includes a small specimen of *Zaraiskites* sp. juv. (cf. *scythicus*) (Fig. 3d), which may indicate the presence of the *Scythicus* Subzone, whereas the upper Bed 24 includes a well-preserved representative of the early *Z. regularis* chronological subspecies with the stage of biplicate ribs preserved in the ontogenesis (Fig. 3h). Similar ammonites occur in the Gorodishche stratotype section beginning approximately from the middle part of the shaly sequence (Rogov, 2005), in the Kashpir section (Fig. 3f), and in northern sections, e.g., the Sysola River basin (Fig. 3g).

Finds of early *Zaraiskites regularis* indicate that the *Panderi* Zone in the Ivkino section also includes the upper *Panderi* Subzone represented by the *Zaraiskites regularis* subsp. nov. faunal horizon. It is conceivable that upper layers of the shale-bearing sequence, which virtually lack ammonites, represent analogues of the *Z. regularis regularis* faunal horizon, because precisely the younger chronological subspecies is relatively abundant in northern areas (Khudyaev, 1927; Repin et al., 2006).

In general, the molluscan assemblage in shales of the *Panderi* Zone is less diverse. It is dominated by small bivalve *Buchia* species, gastropods *Scurria maeotis*, and ammonites largely belonging to the genus *Pavlovia*. Coleoids are rare and represented only by *Acanthoteuthis*. Like coeval sediments of the Gorodishche section (Vishnevskaya et al., 1999), shales are characterized by the prevalence of juvenile molluscan specimens, probably, owing to the unfavorable influence of anoxic environments. At the same time, intercalating beds (for example, Bed 24) include a slightly more diverse assemblage: juvenile forms of ammonites are accompanied by large shells of adult specimens belonging to genera *Pavlovia, Dorsoplanites* (dominant), and *Zaraiskites* (rare).

The palynological analysis of OM from some carbonaceous beds (samples 4,7, 11) revealed that the OM is largely represented by disintegrated algal remains with rare specimens of relatively well-preserved Chorata dinocysts (private communication by G.N. Aleksandrova). Scarcity of dinocysts in the high-carbonaceous sediments is probably explained by some unfavorable

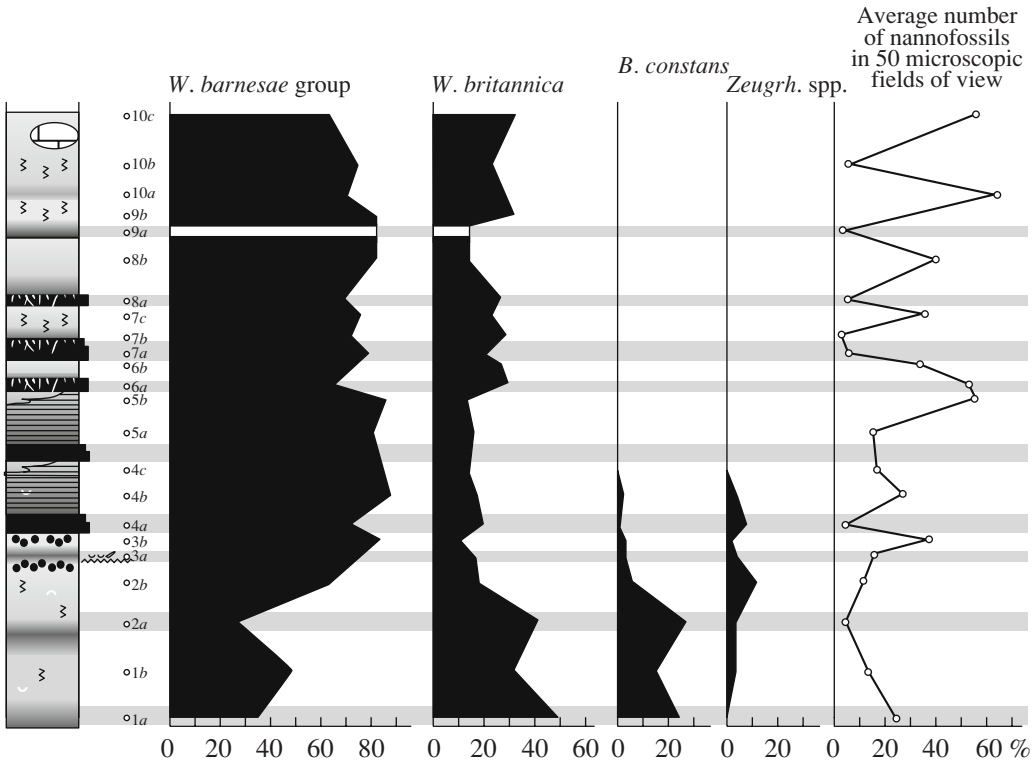

Fig. 5. Distribution of main nannofossil taxa and its total abundance (%) in Kimmeridgian–Volgian sediments of the Ivkino section. For lithological legend, see Fig. 2.

conditions. However, it is rather difficult to identify the unfavorable factor at present.

Results of the Study of Calcareous Nannofossils

Calcareous nannofossils, one of the main components of the Mesozoic–Cenozoic biogenic sedimentation, represents a taxonomically uniform group of unicellular phytoplankton organisms with calcite skeletons of variable morphology. Under favorable conditions, it produces a huge volume of biomass, which promotes high sedimentation rates particularly in epicontinental sea basins. The Jurassic–Cretaceous transition was characterized by high evolutionary rates of nannoplankton, which made it possible to develop the relatively detailed zonations for the Tethyan (Bralower et al., 1989) and boreal (Bown et al., 1988) realms.

The distribution of nannofossils is very irregular in the Ivkino section. The lower part of the section (uppermost Kimmeridgian and Member I of the shale-bearing sequence) is characterized by the high abundance of nannofossils. Their content decreases gradually upward the section (Member II) up to the point of complete disappearance in the upper part (Member III and overlying sandy–silty sediments). Therefore, the results of the statistical analysis are given only for the lower half of the section (Fig. 5). The nannofossil assemblage is largely composed of representatives of the highly tolerant genus *Watznaueria: W. britannica* (Figs. 6a–6c), *W. barnesae* (Fig. 6d), *W. fossacincta* (Fig. 6e), *W. manivitae* (Fig. 6f), *W. ovata* (Fig. 6g), and others, which constitute 70–99% of the assemblage in the lower and upper parts of the sequence, respectively. Such an oligotaxonic composition of the assemblage can be related not only to initially high concentrations of these species, which is typical of Jurassic–Cretaceous sediments worldwide, but also to the fact that and *Watznaueria* spp. are most resistant to dissolution during diagenesis. Therefore, the dominant role of these species can be related to secondary processes, although distinct dissolution signs in nannofossils are noted only in organic-rich beds.

The nannofossil assemblage from the Ivkino section differs substantially from its counterparts in the southern Gorodishche and Kashpir sections of the Ul'yanovsk region (Lord et al., 1987; Kessels et al., 2003) containing frequent the boreal species *Stephanolithion atmetros, Crucibiscutum salebrosum*, and eutrophic forms (*Biscutum constans, Zeugrhabdotus erectus*). In the examined section, the first two species are practically missing. The two last forms (Figs. 6k, 6l) are relatively abundant in the Kimmeridgian sediments and are represented by single specimens in the shale-bearing sequence.

In sediments underlying the shaly sequence, the nannofossils are relatively diverse (up to 10 species) but less abundant: average ~15 species, maximum 25 specimens in the microscopic observation field at a magnifica-

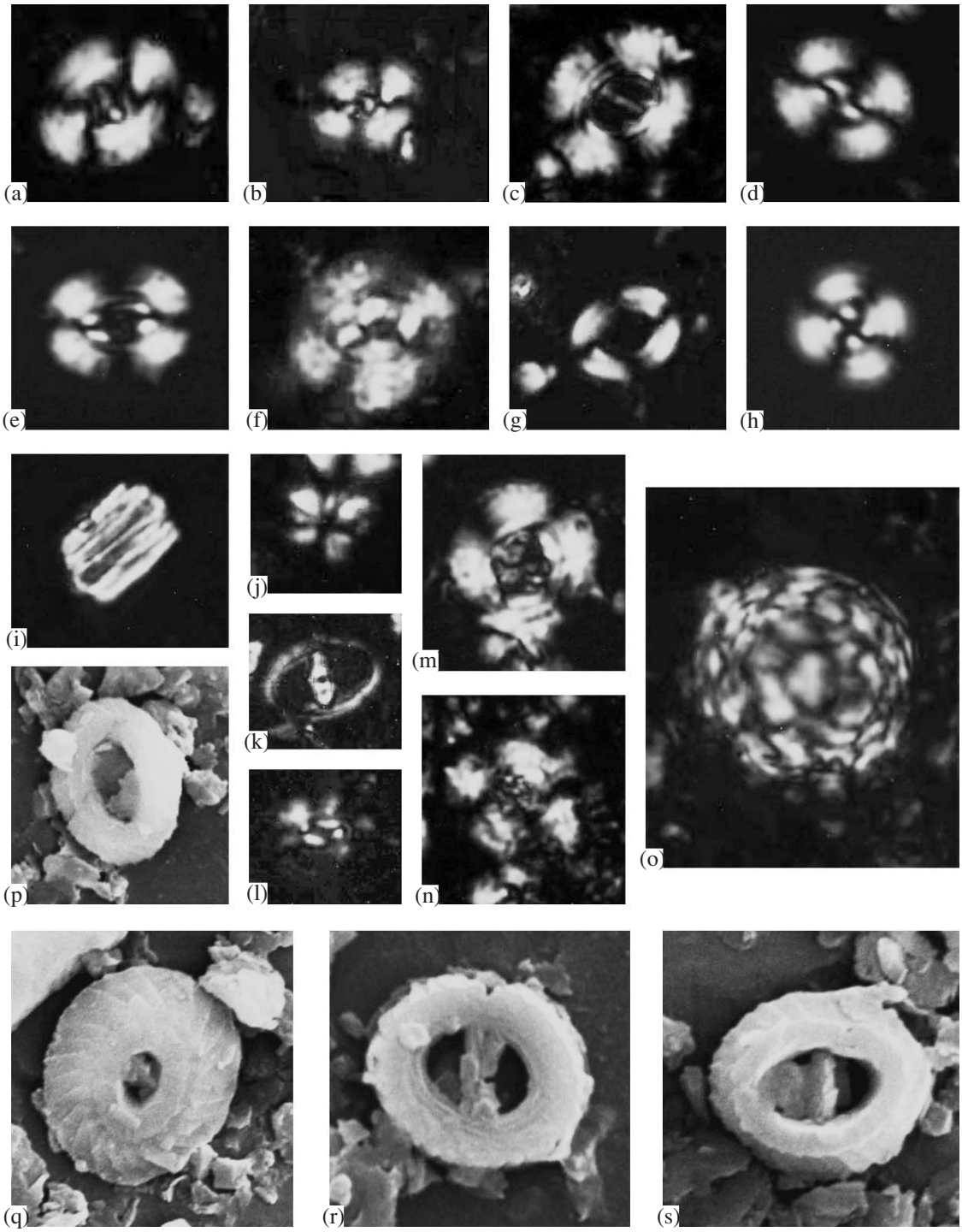

Fig. 6. Photomicrographs of nannofossils from Kimmeridgian–Volgian sediments of the Ivkino section. (a–o) Polarized light, ×6000; (p–s) scanning electron microscope, magn. 12000. (a) typical *Watznaueria britannica* (Stradner, 1963) Reinhardt, 1964, Sample 1*a*; (b) small *W. britannica* sp. specimen with a thick massive placolith and narrow central opening entirely covered by septum, Sample 3*a*; (c) thin large *W. britannica* sp. specimen with a wide central opening and thin septum, Sample 9*b;* (d) *W. barnesae* (Black, 1959) Perch-Nielsen, 1968, Sample 1*a*; (e) *W. fossacincta* Wind and Cepek, 1979, Sample 1*b*; (f) *W. manivitae* Bukry, 1979b, Sample 4*b*; (g) *W. ovata* Bukry, 1969b, Sample 6*a*; (h) *Cyclagelosphaera margerelii* Noël, 1965, Sample 2*a*; (i) *Conusphaera mexicana* Trejo, 1969, Sample 3*a*; (j) *Polycostella beckmannii* Thierstein, 1971, Sample 6*a*; (k) *Zeugrhabdotus erectus* (Deflandre *in* Deflandre and Fert, 1954) Reinhardt, 1965, Sample 9*b*; (l) *Biscutum constans* (Gorka, 1957) Black *in* Black and Barnes, 1959, Sample 4*a*; (m) *Microstaurus chiastius* (Worsley, 1971) Grün *in* Grün and Allermann,1975, Sample 20*b*; (n) *M. chiastius*, Sample 10*b*; (o) coccosphaera of *Watznaueria* sp., Sample 4*b*; (p) *W. ovata*, Sample 2*a*; (q) *W. fossacincta*, Sample 2*a*; (r) *W. britannica*, proximal disc, (s) *W. britannica*, distal disc.

tion of 1250. The assemblage is largely composed of numerous *Watznaueria barnesae, W. britannica, Cyclagelosphaera margerellii* (up to 25%), and rare *Biscutum constans* (up to 11%) (Fig. 6). Such an assemblage is characteristic of normal marine (probably, mesotrophic) environments. Of stratigraphic significance is only the find of single *Hexapodorhabdus cuvillieri*, which disappears at the upper Kimmeridgian boundary.

Conusphaera mexicana (Fig. 6i), which marks the lower boundary of Zone NJ20A (middle Tithonian or upper part of the lower Volgian Substage), appears at the base of the shale-bearing sequence above the lower phosphorite horizon (Sample 3a). The slightly higher horizon (Sample 6) includes *Polycostella beckmanni* (Fig. 6j), which marks the base of Subzone NJ20-B (Fig. 2), and *Microstaurus chiastius* (Figs. 6m, 6n), which marks the lower boundary of Zone NJK-A (uppermost middle–basal upper Tithonian, uppermost lower–basal middle Volgian). Thus, it can be assumed that the base of the third black shale bed coincides with hiatus corresponding to Subzone NJ20B. It should be taken into consideration, however, that the above-mentioned species are abundant in the Tethyan realm and scarce in the examined section. Therefore, their appearance levels in the study region may slightly differ from the true evolutionary appearance; i.e., the real age of sediments may be slightly older than that indicated by nannoplankton. It is remarkable that the high-latitude Ivkino section contains (although scarce) warm-water forms, which define zonal units of the Tethyan scale corresponding to the middle Tithonian Substage. Their occurrence in this boreal section is most likely related to a complex system of currents in the shallow Central Russian Basin.

The nannofossil assemblage from the lower part of the shale-bearing sequence, which is compositionally similar to that in the underlying Kimmeridgian sediments, shows a notably lower abundance of eutrophic taxa and a prevalence of *Watznaueria* spp. The basal layers contain *Cyclagelosphaera margerellii* (Fig. 6h) and *Biscutum constans*, which are practically missing above the second shale interbed. Beginning from this level, the content of all nannofossil taxa, except *Watznaueria* representatives, does not exceed 1%. In carbonaceous shales, abundance of nannofossils decreases sharply, while they are abundant and play the rock-forming role in the adjacent carbonate interbeds (Fig. 5). The population of different representatives of *Watznaueria* species demonstrates notable changes. In the Kimmeridgian assemblage, taxa lacking the central opening or with a small opening without central bridge, e.g., *W. barnesae, W. fossacincta, W. ovalis, W. manivitae* (Figs. 6d–6g), which are conditionally united into the *W. barnesae* group, and forms with a more or less wide central opening divided by the central bridge (*W. britannica*; Fig. 6) occur in equal proportions. In contrast, the assemblage from the lower part of the shale-bearing sequence is dominated by taxa of the first group, the population of *W. britannica* is drastically decreased, and its content slightly increases only in some carbonaceous layers. In the basal part of Volgian sediments, the *W. britannica* group is divided distinctly into two morhotypes. Morphotype 1 (*W. britannica* sp. 1, Figs. 6b, 6o) is represented by small massive forms with a small central opening almost closed by central bridge. Morphotype 2 (*W. britannica* sp. 2, Fig. 6c) is characterized by large thin coccoliths with a wide central opening; i.e., they are less calcified. No transitional forms are observed between these morphotypes, suggesting that the taxon likely attempted to adapt to substantially different ecological niches. It is conceivable that they dwelt at different depths of the basin and the significant differentiation of planktonic forms is related to the strong stratification of its water column. Higher in the section, the share of thin large *W. britannica* sp. 2 with the wide central opening is notably higher. This is sometimes interpreted as indicator of some warming (Giraud et al., 2006) and deficiency of Ca in the basin. In the overlying sample 10 (Figs. 2, 5), the amount of nannofossils decrease sharply and disappears completely above sample 21. Only sample 24 contains an abundant nannofossil assemblage composed largely of *W. fossacincta*, which is less calcified than *W. barnesae.*

The results of the statistical analysis of nannofossil assemblages from the Ivkino section differ from the data obtained for coeval assemblages from the lower latitudes of the Atlantic (Bornemann et al., 2003; Tremolada et al., 2006). In the Atlantic region, the upper part of Subzone NJK-A demonstrates a sharp increase in species diversity of nannofossils and an abundance of strongly calcified massive forms *Cornusphaera mexicana, Polycostella beckmannii*, and *Nannoconus* spp. In the Ivkino section, these taxa occur as single specimens in the lower part of the shale-bearing sequence. These data indicate different concentrations of dissolved Ca in waters of oceanic and epicontinental basins in the terminal Jurassic. In oceans, its content was sufficient to provide high productivity of strongly calcified taxa, while epicontiental seas were populated by forms that consumed minimal concentrations of dissolved calcium carbonate for the formation of skeletons.

Enhanced eutrophication of the basin affected negatively the nannoflora and provoked the extinction of most taxa, including the eutrophic forms that could tolerate only an insignificant eutrophication. The released ecological niches were occupied by the most tolerant taxa that could tolerate significant changes in environmental parameters.

Glauconite-bearing sandy–silty sediments overlying the shaly sequence in the examined section (Fig. 2) lack ammonites and nannofossils. Therefore, the reliable dating of such sediments is rather difficult. It should be noted that lithologically similar sediments overlying the shale-bearing sequence with an erosional surface in other areas of the Moscow Basin can be correlated with either the *Virgatites virgatus* Zone of the Volgian Stage, which is defined as the Egor'evsk For-

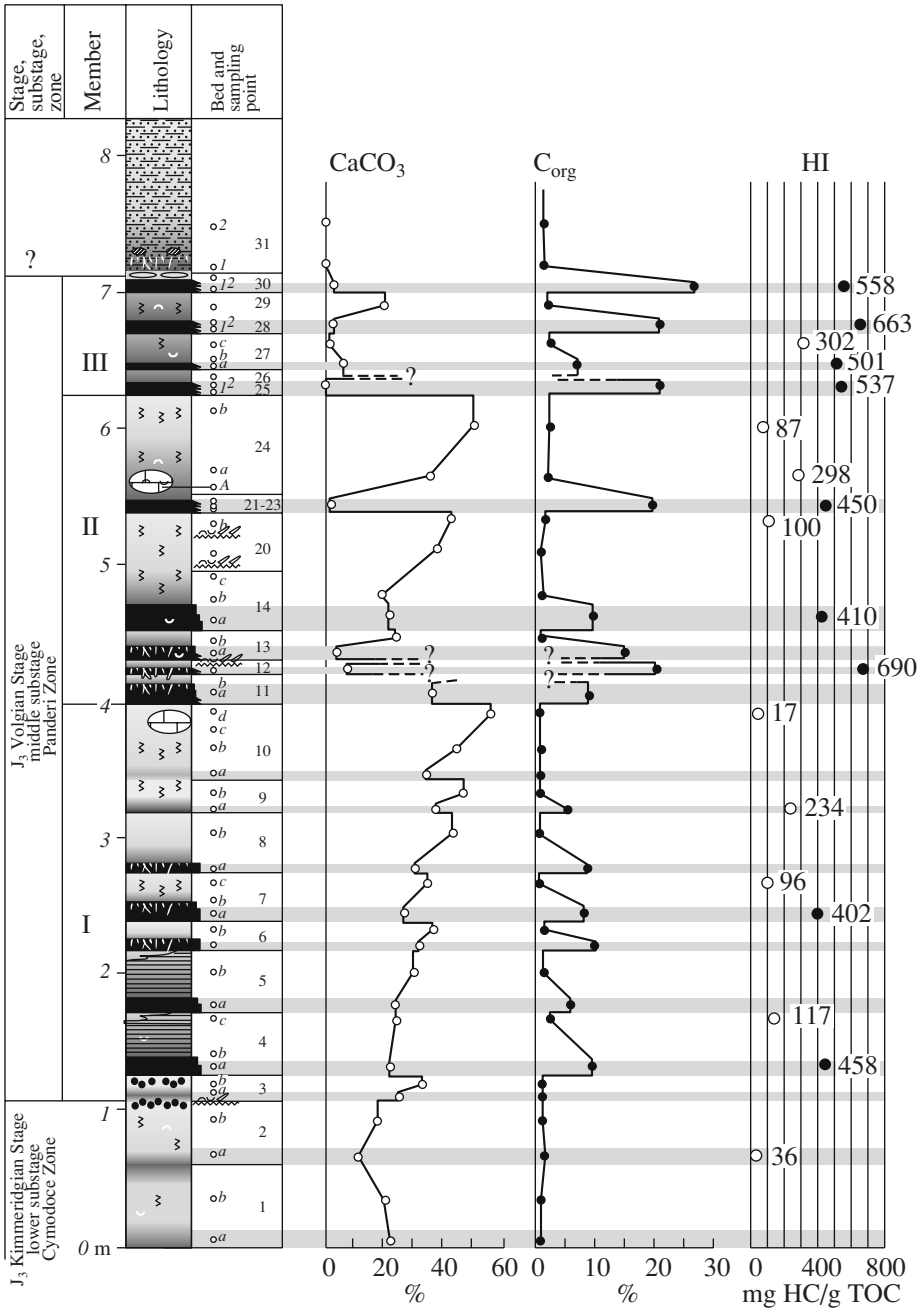

Fig. 7. Distribution of C_{org}, $CaCO_3$, and hydrogen index (HI) in sediments of the Ivkino section (based on OM pyrolysis data). In the HI column, solid and open circles designate oil shales and calcareous clays, respectively.

mation according to (Olfer'ev, 1986), or the lower Valanginian (Gerasimov et al., 1982).

LITHOLOGICAL CHARACTERISTICS OF SEDIMENTS

Figure 7 illustrates lithological column of the Ivkino section with the distribution of C_{org} and $CaCO_3$ and variations of the hydrogen index (HI) based on the pyrolytic analysis of OM.

Lower Kimmeridgian Sediments

Lower Kimmeridgian sediments (apparent thickness ~1.2 m) are represented by alternation of the relatively dark gray and notably lighter beds (a few tens of centimeters thick) of calcareous clays ($CaCO_3$ 11–33%). The clays contain an admixture of silty material (10–20%) (Figs. 8a, 8b).

Couplets of differently colored beds make up cyclites. Their dark and light sediments should be con-

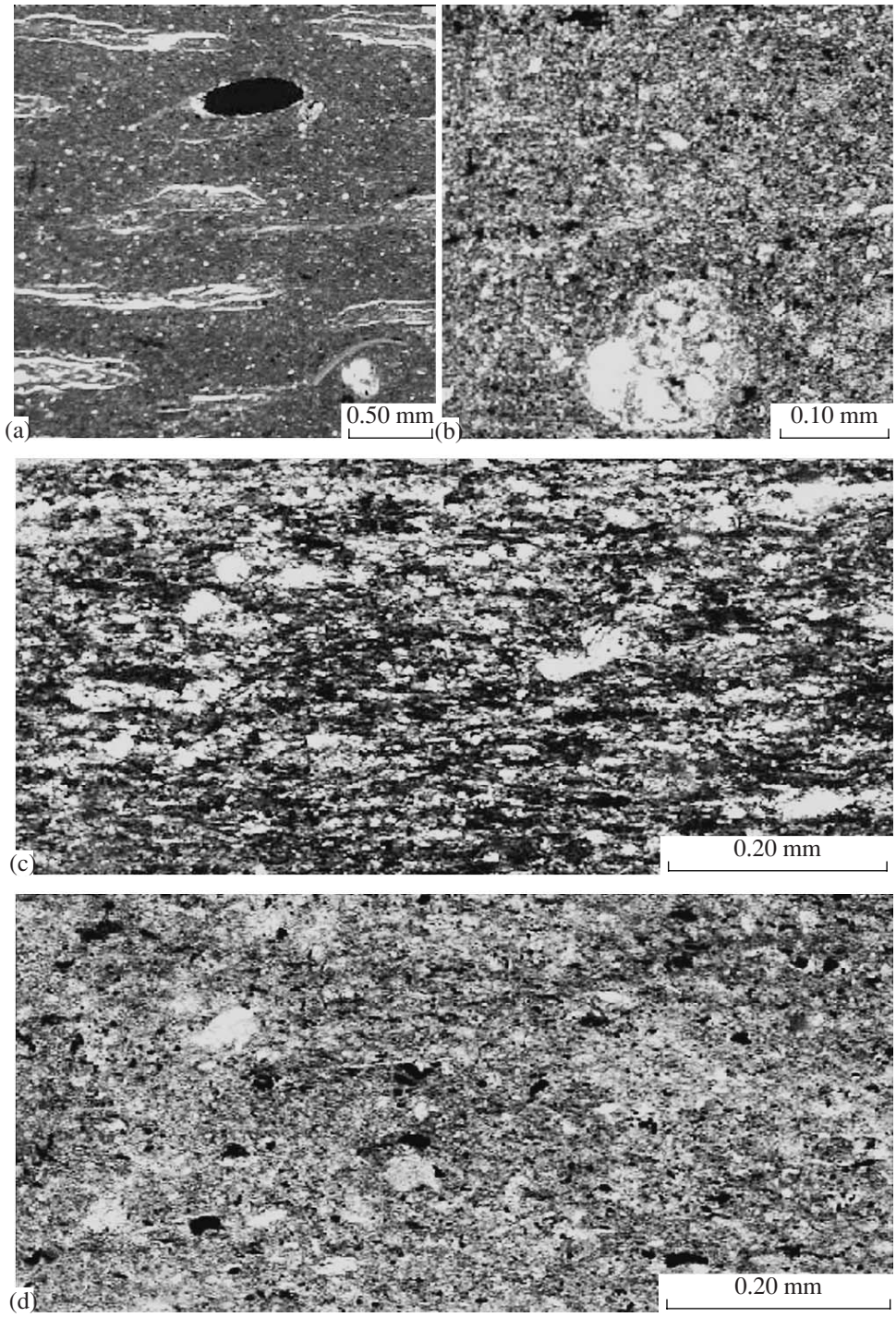

Fig. 8. Microtexture of sediments in the Ivkino section. (a, b) Lower Kimmeridgian calcareous clays: (a) rocks with bioturbation signs from the lower part of a cyclite, Sample 1*a* (white and black correspond to fucoids filled with sediments and pyrite, respectively), (b) rocks from the upper part of a cyclite, Sample 2*b* (OM is practically missing); (c–f) rocks from different parts of a cyclite in the shale-bearing sequence: (c) carbonaceous shale from the lower part of a cyclite, Sample 4*a* from Member I (dark zones are small colloalginite lenses), (d) light calcareous clays from the upper part of the same cyclite, Sample 4*c* (black zone is a small plant detritus), (e) high-carbonaceous oil shales from the lower part of a cyclite, Sample 28*a* from Member III (dark and gray zones are colloalginite lenses and laminae, respectively), (f) low-carbonate clays from the upper part of the same cyclite, Sample 28*b* (dark zone is finely dispersed OM; (g, h) sandy–silty sediments overlying the shale-bearing sequence: (g) bioturbation structure of sandy–silty rocks (dark zone is clayey matrix, while light zones are transverse sections of fucoids filled with silty glauconite–quartz material), (h) glauconite in sandy–silty rocks.

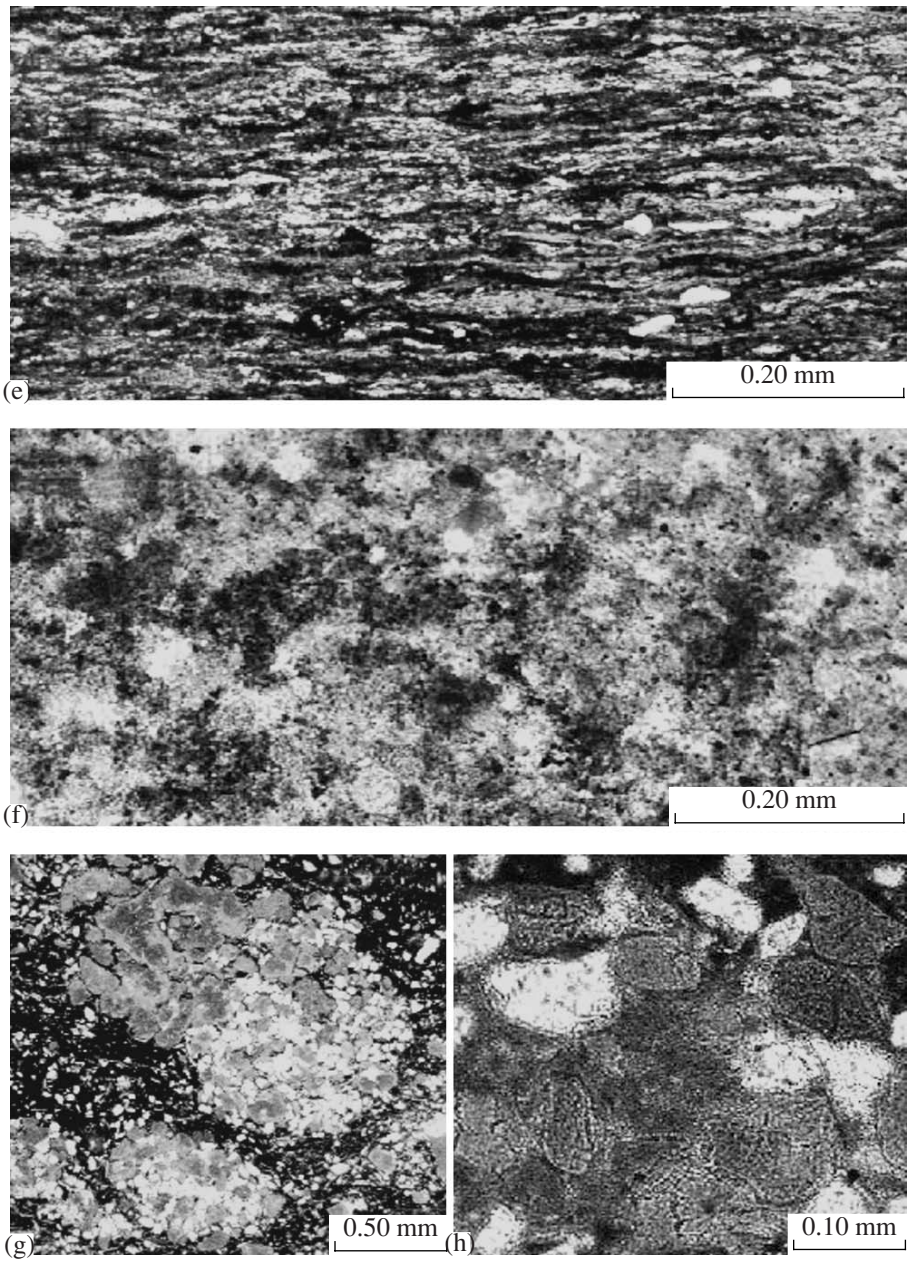

Fig. 8. (Contd.)

sidered the lower and upper elements, respectively, because transition from the dark sediments to the light variety is gradual, whereas transition from the light layer to the dark layer is relatively sharp. This part of the section includes two such cyclites (0.75 and 0.45 m). Each of them demonstrates upsection increase in the carbonate content and decrease in the C_{org} content (Fig. 7).

The lower Kimmeridgian sediments are characterized by platy jointing and negligible sedimentary lamination. Fucoids of burrowing organisms occur as subhorizontal thin slightly curved tubes up to 1–2 cm long. Thin sections show that the fucoids are largely filled with clayey material that is similar to the groundmass but more compact. The sediments contain mainly small molluscan shells. Morphological uniformity of fucoids and low content of benthic fossils indicate unfavorable conditions for dwelling of the benthos at the bottom of the early Kimmeridgian basin. Development of reducing environments in the bottom sediments is evident from numerous sulfide aggregates, which fill cavities of shells and fucoids (Fig. 8a) and make up a regular dissemination of microframboids.

The lower Kimmeridgian section is crowned by a phosphoritic conglomerate bed (0.08 m) consisting of dark phosphate nodules (up to ~5 cm across) and their small angular fragments of the gravel–sand size. It also encloses rostra of small belemnites and fragments of small ammonite shells.

Table 1. Concentrations of chemical elements in sediments of the Ivkino section

Age	Sample	C_{org}	$CaCO_3$	Fe	Mn	Ti	P	S	Cr	V	Ni	Co
J_3, lower Kimmeridgian	1*a*	0.98	22.7	4.03	0.053	0.44	0.05	0.75	120	132	151	86
	1*b*	1.00	21.00	4.4	0.038	0.46	0.05	1.02	137	142	115	92
	2*a*	1.59	11.58	4.85	0.036	0.53	0.08	–	135	157	239	94
	2*b*	1.09	18.05	4.76	0.046	0.48	0.06	1.79	136	247	470	170
J_3, Volgian Stage, middle substage, *Panderi* ammonite zone	3*a*	1.09	25.54	3.71	0.044	0.39	0.08	0.77	99	170	530	175
	3*b*	1.03	33.03	3.07	0.357	0.37		–	78	125	292	92
	4*a*	9.40	22.36	3.18	0.034	0.34	0.12	–	111	182	112	29
	4*b*	3.00	16.34	3.49	0.032	0.46	0.07	–	106	132	109	30
	4*c*	2.46	24.52	3.17	0.032	0.42	0.06	–	103	115	101	31
	5*a*	5.80	23.84	2.78	0.032	0.35	0.05	–	123	160	94	26
	5*b*	1.34	30.08	2.97	0.044	0.37	0.04	–	92	101	242	120
	6*a*	9.90	32.12	2.67	0.039	0.33	0.05	–	98	107	135	68
	6*b*	1.30	36.77	2.94	0.044	0.39			92	78	230	100
	7*a*	7.95	27.13	2.53	0.036	0.28	0.12	–	104	182	84	23
	7*b*	7.80	26.11	3.16	0.046	0.28	0.09	–	102	137	103	44
	7*c*	0.51	34.50	2.69	0.034	0.35	0.06	–	102	150	98	31
	8*a*	8.50	30.65	2.76	0.035	0.26	0.11	_	88	155	107	23
	8*b*	0.52	43.24	2.4	0.075	0.3	0.05	–	84	88	257	100
	9*a*	5.20	37.46	2.64	0.054	0.29	0.05	–	88	90	110	33
	9*b*	0.57	46.54	2.27	0.096	0.28	0.05	–	71	61	203	76
	10*a*	0.62	34.39	2.85	0.048	0.37	0.05	–	82	85	196	61
	10*b*	0.68	44.27	2.28	0.056	0.27	0.03	–	73	78	155	43
	10*c*	0.40	55.62	2.1	0.106	0.22	0.06	–	61	54	170	35
	11	8.70	36.32	2.53	0.048	0.18	0.12	–	67	127	81	16
	12	20.10	7.49	3.79	0.03	0.27	0.18	–	114	450	94	28
	13*a*	14.80	3.75	4.9	0.037	0.32	0.16	–	162	760	110	29
	14*b*	9.40	21.68	3.47	0.027	0.28	0.15	–	105	440	107	22
	14*c*	0.82	19.07	3.99	0.034	0.38	0.08	–	107	145	114	35
	20*a*	0.68	37.68	2.61	0.055	0.29	0.04	–	82	88	137	36
	20*b*	1.36	42.34	2.88	0.039	0.31	0.07	–	76	75	74	25
	21	12.20	0.91	5.96	0.032	0.38	0.23	2.64	145	760	135	32
	22	15.60	3.41	6.29	0.036	0.31	0.32	1.89	136	1000	132	35
	23	19.30	1.93	5.27	0.033	0.32	0.34	2.56	132	1070	135	35
	24*a*	1.8	35.19	3.55	0.054	0.34	0.12	–	103	152	125	58
	24*b*	2.16	4.77	4.9	0.037	0.32	0.16	0.69	127	240	212	91
	25-*2*	20.5	0.03	3.89	0.018	0.32	0.19	4.32	142	580	160	37
	26	21.5	0.45	3.84	0.019	0.3	0.25	4.30	143	640	151	32
	27*a*	6.5	5.90	5.15	0.026	0.44	0.23	2.91	157	350	155	51
	27*b*	7.9	7.60	4.39	0.027	0.39	0.27	2.52	130	310	145	48
	27*c*	2.13	2.04	4.97	0.051	0.47	0.43	0.87	109	282	140	56
	28-*1*	13	0.03	4.65	0.023	0.36	0.05	4.64	144	600	172	76
	28-*2*	20.4	2.38	3.26	0.02	0.29	0.04	–	130	1200	252	73
	28-*3*	27	2.61	3.32	0.016	0.31	0.11	–	124	1100	210	55
	29	1.79	19.52	13.45	0.339	0.37	0.16	0.78	100	205	219	76
	30	26.2	2.72	3.03	0.0068	0.18	0.19	–	120	1000	315	125
?, overlying sediments	31-*1*	0.98	None	7.44	0.013	0.5	0.13	–	130	290	53	28
	31-*2*	1.01	None	6.91	0.014	0.47	0.14	0.24	145	325	64	35

Note: Contents of C_{org}, $CaCO_3$, Fe, Mn, Ti, P, S, SiO_2, and Al_2O_3 are given in %; others, in ppm. (–) Not determined.

Cu	Pb	Zn	Mo	Ag	As	Hg	Sn	Ga	Ge	B	SiO_2	Al_2O_3
37	22	147	3.8	0.08	7.4	0.10	3.7	11	1.5	54	40.51	13.87
31	14	92	2.8	<0.08	7.4	0.11	3.8	11	1.4	54	41.76	13.36
42	17	140	3.5	0.09	7	0.07	3.6	11	1.5	54	45.00	15.26
57	19	245	6.0	0.34	15	0.10	3.7	10	1.3	52	41.19	13.86
65	33	320	2.4	0.2	15	0.11	3	7	1.3	57	36.38	12.41
42	40	225	4.0	0.13	13	0.12	3.1	8	1.1	48	34.27	12.21
70	18	60	11	0.23	15	0.06	2.7	6	0.5	46	30.78	11.52
87	30	122	5.6	0.16	6	0.08	3.4	12	1.1	58	42.93	15.05
76	30	127	5.0	0.14	8.1	0.06	3.1	12	1.2	62	41.12	14.16
78	18	70	7.0	0.22	5.5	0.09	3.8	9	0.5	51	34.84	12.76
52	36	145	3.3	0.13	12	0.06	3.4	11	1.1	52	36.94	13.1
63	28	125	3.4	0.14	7.5	0.09	3.1	9	1.1	51	34.27	12.00
47	30	140	2.6	0.1	13	0.06	3.4	11	0.7	51	36.78	12.92
72	16	50	9.6	0.22	4.1	0.08	2.3	4	0.7	46	29.61	10.05
45	12	40	4.3	0.16	10	0.08	2	4	<0.3	40	28.57	9.33
57	27	105	6.6	0.17	3.6	0.08	3.1	8	1	49	33.53	10.72
54	13	?	6.0	0.21	5.7	0.10	2.3	3	<0.3	37	25.39	8.84
45	31	205	4.0	0.15	4.1	0.1	2.9	7	1.1	48	29.96	9.81
35	16	53	5.0	0.13	4.3	0.10	2.5	5	<0.3	40	27.03	9.15
31	27	125	3.0	0.1	<3	0.09	3	5	0.5	41	27.45	9.19
47	37	220	2.6	0.13	5.3	0.10	2.8	8	1.1	57	35.85	11.9
37	29	140	3.6	0.09	<3	0.10	2.6	6	0.7	48	28.21	8.72
42	20	135	1.2	0.16	<3	0.11	2.6	4	0.7	41	23.11	7.84
45	11	?	12	0.17	5.6	0.10	<1.5	3	0.4	36	20.18	6.63
57	14	60	33	0.2	7.8	0.10	2.7	5	0.4	44	27.05	9.09
78	17	105	26	0.25	11	0.10	3.4	11	0.5	48	32.58	10.74
78	15	105	30	0.31	11	0.08	2	11	0.8	48	29.58	9.54
72	30	160	8.1	0.1	9.3	0.11	3.6	11	1.3	70	40.41	14.23
43	30	180	5.0	0.08	3.9	0.10	2.9	10	0.7	54	32.94	11.5
40	22	125	4.0	0.09	3.3	0.08	2.6	7	0.8	48	29.56	11.07
100	23	220	37	0.42	12	0.11	3.4	8	1.3	52	36.66	12.24
118	22	285	42	0.7	21	0.11	3.9	6	1.5	54	32.9	10.86
146	26	340	58	0.63	13	0.11	4.3	12	1.5	54	33.32	11.83
47	20	165	11	0.13	7.7	0.08	3.5	12	1	62	32.46	11.97
75	31	300	11	0.18	8.7	0.09	4.5	9	1.5	82	50.3	17.57
100	24	480	110	0.32	17	0.10	3.8	11	1.5	62	31.28	10.54
95	20	415	100	0.32	15	0.10	3.6	9	1.4	58	31.13	10.82
98	22	210	25.5	0.24	23	0.10	4.3	4	0.8	60	43.47	14.36
73	21	300	34	0.22	23	0.10	3.7	4	1.3	67	42.63	15.1
78	33	400	10.3	0.15	15	0.08	3.9	8	1.4	84	50.34	17.01
103	23	220	43	0.34	79	0.11	4.8	3	0.4	57	34.8	12.03
120	31	670	130	0.52	48	0.09	3.6	7	1.3	54	30.45	11.58
120	31	490	140	0.46	53	0.08	3.3	5	1.3	56	29.22	11.26
45	15	165	8.8	0.09	12	0.08	4.8	5	0.8	40	40.00	13.95
105	15	740	160	0.33	100	0.08	4.8	8	1.4	44	18.13	7.45
35	20	82	6.8	0.2	4.8	0.08	4.5	6	1.9	91	56.85	12.33
28	27	79	6.5	0.16	18	0.08	4.6	4	2.3	88	58.11	12.85

The conglomerate is overlain by a dark gray clay bed (0.17 m) with inclusions of black angular phosphate and glauconite grains of the gravel–sand size. The clay bed is overlain by another thin (0.02–0.03 m) bed of phosphoritic conglomerate (Fig. 4). As was mentioned, the clayey rock and conglomerate bed is attributed to the basal layer of the middle Volgian Substage.

Middle Volgian Sediments of the Panderi Zone

Structure of the shale-bearing sequence. The sequence is characterized by distinct cyclic pattern with at least 17 cyclites. The complete elementary cyclite consists of three elements (Fig. 7, samples 7a–7c, 8a, 8b, 21–24b, and others). The lowest element is represented by high-carbonaceous rocks (shales), while the middle and upper elements are composed of the dark and light carbonate clays, respectively (Figs. 8a–8f). However, rocks of the middle (darker) element are usually enriched in C_{org} and depleted in $CaCO_3$ as compared with the upper (lighter) element. Some cyclites are lacking the upper (lightest) layer. The lower shaly layer is absent in rare cases (Fig. 7, samples 10a–10c, 20a–20c). Boundary between the cyclites is sharp and distinct at the base of the shaly layer, while others transitions are more gradual and considered as internal boundaries.

The elementary cyclites in the shale-bearing sequence are grouped into three members.

The lower Member I (2.8 m thick) unites seven cyclites (Fig. 7, samples 4–10) with the thickness of individual cyclites up to 0.5 m or more in some cases. Table 1 shows that the C_{org} content in shales does not exceed 12% and is minimal for the shale-bearing sequence (samples 4–10). In contrast, the $CaCO_3$ content in these rocks (particularly, in the upper elements of cyclites) is highest for the sequence and increases upsection from 22 to 55%.

The middle Member II (1.7 m) comprises six cyclites with an irregular distribution of shale beds (Figs. 2, 7). The lower part of the member includes three cyclites, in which the middle element is reduced and the upper element is absent. The thickness of cyclites does not exceed 10–15 cm. In contrast, the overlying two cyclites are substantially thicker (0.7 m or more). Moreover, the lower cyclite can be subdivided into two smaller cyclites. One of them includes only the middle and upper elements. The second member with irregular cyclic patterns encloses several erosional surfaces (condensation horizons). Relative to the lower member, the C_{org} content in shales from the middle member is notably higher (almost 27%). The $CaCO_3$ concentration remains relatively high and shows a slight decrease in the uppermost part of the member.

Boundaries between the lower and middle members are drawn at the roof of the relatively thick light gray calcareous clays.

The upper Member III (0.7 m) unites four cyclites each 0.2 m thick. The uppermost cyclite is reduced likely due to erosion of its upper part. All cyclites of this member are lacking the upper element (light calcareous clay). The C_{org} content in shales from this member is maximal (20–26%), while the $CaCO_3$ concentration is significantly lower as compared with the remaining part of the section.

No distinct cyclicity is observed in sandy siltstones (apparent thickness ~5 m), which overlie the shale-bearing sequence with a sharp boundary.

Lithology of the shale-bearing sequence. Despite the apparent similarity of different parts of the shale-bearing sequence, its lithology shows notable variations through the section.

In the lower part of Member I (~1.2 m), carbonaceous shales (Fig. 8c) are dark gray with brownish tint. Their bedding surfaces contain rare small thin-walled bivalve shells and abundant small carbonate and phosphate biogenic detritus.

Both shales and clayey sediments demonstrate thin horizontal lamination related to the alternation of laminae enriched in OM or carbonate material (CM). Lamination is irregularly bioturbated (locally up to 50 vol %). Bioturbation patterns indicate that the sediments were intermittently reworked by small burrowing organisms in the uppermost (a few centimeters thick and substantially water-saturated) layer. Therefore, sediments of this member are lacking morphologically distinct ichnofossils.

Clayey sediments from the upper part of Member I are characterized by a notably higher carbonate admixture, lighter color, and more contrasting differences between the lower and upper parts of cyclites. Faunal remains are more abundant and diverse. They are frequently represented by intact shells of bivalves, gastropods, and small (several centimeters across) ammonites. The fossils are accumulated along bedding surfaces of shales. One can also see numerous small trails of *Chondrites* and solitary subhorizontal ribbon-shaped meandering trails of *Planolites* (up to 10 cm long and ~0.5 cm across). Both trails are filled with lighter material.

Calcareous clays in the upper parts of cyclites are almost entirely homogenized by bioturbation (Fig. 8d). Therefore, they have a massive homogenous texture.

Dark gray clay interbeds separating the carbonaceous shales and light clayey–calcareous sediments within the elementary cyclites show transitional characteristics. They are usually enriched in C_{org} and $CaCO_3$ (Table 1). These interbeds, particularly their upper parts, are saturated with small fucoids (*Chondrites, Planolites*, and others are most abundant). They are well distinguished owing to their sedimentary infill represented by light material similar to that in the overlying sediments. Fucoids show distinct external boundaries and preserve their fine morphological features. According to (Bromley, 1996; Mikulash and Dronov, 2006), such ichnofossils are formed in plastic sediments that can retain fine morphological features of traces of life activity. They could be left either by organisms that populated slightly lithified sediments

and were exhumed owing to the erosion of the overlying beds or by infauna that dwelt in the relatively deep horizons of sediments and crosscut lithological boundaries (the lower bioturbation level).

Member I is crowned by a bed of large lenslike concretions (~1 m across, ~0.3 m thick) composed of homogenous microcrystalline calcite.

In Member II, carbonaceous shales are characterized by thin platy uniform jointing and slight bioturbation. Traces of biogenic reworking are usually rare. They are usually distinguished in thin sections owing to peculiar small (a few millimeters long) subvertical funnel-shaped holes, cracks, and bends in the laminae. It is conceivable that accumulation of carbonaceous sediments was accompanied by the episodic dwelling of mobile (mostly small) organisms or meiofauna according to (Bromley, 1996). Bedding surfaces of shales in this member contain accumulations of deformed shells of bivalves, gastropods, and small ammonites, as well as shelly detritus, rare small *Chondrites* fucoids and single ribbon-like meandering trails of crustacean (?).

Upper parts of cyclites in this member are composed of light gray homogenous bioturbated clayey–calcareous sediments that are lithologically similar to their counterparts from the underlying member.

In contrast to Member I, the section of Member II often contains cyclites with significantly reduced thickness or without the upper clayey parts. Intermittent erosion of sediments is evident from the presence of interbeds with numerous fragments of belemnite rostra and shelly detritus. It should be noted that belemnite remains are generally rare in the sequence and are mainly confined to these interbeds.

Dark clays in the middle element of the upper cyclite of Member II host a bed of lenslike calcareous concretions (up to 0.3 m across and 0.15 m thick). The concretions of microcrystalline calcite are characterized by fine lamination, which is almost destroyed in the host sediments due to bioturbation. The concretions were formed rather rapidly at the earliest diagenetic stage: in contrast to host sediments, they are lacking notable traces of distortion by the infaunal organisms.

Member III encloses shale varieties with the maximal C_{org} and minimal $CaCO_3$ contents. In terms of properties, the sediments correspond to the term "oil shale." The associated clayey sediments are characterized by the lowest $CaCO_3$ contents in the entire sequence (Table 1, Figs. 8e, 8f).

Shales in this part of the sequence differ from the underlying varieties even by their appearance—rocks consisting of frequently alternating laminae (a few centimeters thick) of laminated and organic-rich oil shales (C_{org} up to 20% or more) and more massive beds of clayey–silty material (C_{org} 6.5–13.0%). In the oil shale laminae, clay particles, OM aggregates, and other components are oriented parallel to bedding surfaces and signs of bioturbation are absent. In contrast, clayey–silty laminae demonstrate numerous small biogenic distortions of bedding as funnel-shaped holes filled with silty material, which are readily distinguishable in thin sections.

The uppermost part of the shaly sequence encloses a bed of dark brown uniform thin foliated oil shales (0.10–0.12 m thick) with the C_{org} content up to 26%. The shales are readily separated into thin (a few millimeters) laminae with bedding surfaces lacking any faunal remains. Thin sections show that OM in the rock is concentrated in thin frequent laminae and is represented by brownish yellow amorphous colloalginite (Fig. 8e).

The upper parts of reduced cyclites of Member III are composed of greenish gray low-carbonate massive clays with admixture of silty material (up to 10%). These sediments contain small tubular fucoids (up to 0.5 mm in diameter) frequently filled with pyrite and uniform dissemination of brown microspherulites composed of iron hydroxides (oxidized pyrite framboids). One can also see rare pyrite aggregates (up to 2 cm across) with shapes indicating their formation within molluscan shells.

Fossils in carbonaceous sediments of Member III are represented by single finds of ammonite and large bivalve (inocerams and buchias) conchs. The bivalves are dissolved to a variable extent and sometimes only their impressions are preserved. Clays contain a small amount of faunal remains and rare fragments of large carbonate shells.

The upper part of the finely foliated shales crowning the shale-bearing sequence is cemented by phosphate material and traced within the outcrop as a thin (up to 5 cm) continuous light brown bed. Thin sections demonstrate a distinct sedimentary texture of the carbonaceous material cemented by a colloform phosphate matter (francolite and hydroxylapatite). The surface of the phosphate bed is uneven hummocky, and, probably, bioturbated. Depressions are filled with an incoherent greenish gray sandy–silty material, which is compositionally similar to the sediments overlying with an erosion.

As follows from this description, the main rock-forming components of the shale-bearing sequence are represented by terrigenous (carbonate) and biogenic (organic) material with the subordinate admixture of authigenic sulfide, silicate, and phosphate aggregates.

The terrigenous material consists of clay minerals with silty admixture (quartz with the subordinate feldspar, mica, and glauconite), which constitutes an insignificant share of sediments and rarely exceeds 10%.

We studied a series of samples taken from different parts of the section to study the mineral composition of clays. The X-ray diffraction analysis revealed that fraction <0.001 mm is mainly composed of smectite, mixed-layer mica–smectite minerals (up to 30% of micaceous layers), hydromicas (5–10% of swelling interlayers), kaolinite, and the subordinate chlorite.

The constant mineral composition and proportions of the main components in the clay fraction of sediments is a characteristic feature of the Ivkino shale-bearing sec-

tion. The pattern is slightly different in coeval sediments of the middle Volga region. For example, the upper part of the shale-bearing sequence in the Gorodishche section demonstrates a drastic decrease in the content of kaolinite (up to the point of its complete disappearance) accompanied by the increase in the smectite content and the appearance of clinoptilolite as one of the rock-forming components (Shimkyavichus, 1986; Ruffell et al., 2002; Riboulleau et al., 2001; original data).

Like in the underlying lower Kimmeridgian strata, carbonate material in the middle Volgian sediments is represented by the finely dispersed calcite (based on microscopic and X-ray spectroscopic studies). The biogenic CM consists of irregularly distributed calcareous nannoplankton skeletons and small fragments of molluscan shells. The $CaCO_3$ content in clays of Member I increases upward the section and reaches 55% in its uppermost part (Table 1, Fig. 7). The carbonaceous shales also show a high content of the calcareous admixture.

Member II is characterized by the permanently high content of $CaCO_3$ in the clayey sediments and its significant variation in different cycles within the carbonaceous shales. In Member III, CM is insignificant in the alternating carbonaceous shales (with variable C_{org} concentrations) and clays. Hence, this sedimentation stage was marked by significant ecological changes in the paleobasin and the consequent sharp reduction of the productivity of calcareous organisms.

Comparison of the distribution of $CaCO_3$ and C_{org} in the shale-bearing sequence revealed a negative correlation between these components: increase in the content of one component is accompanied by decrease in the concentration of another component (Table 1, Fig. 7), although this correlation is expressed in variable extent.

Organic matter occurs in different forms in carbonaceous shales and clays.

Carbonaceous shales are dominated by the amorphous OM (up to 90–99%) corresponding to colloalginite according to terminology in (Ginsburg, 1991). Colloalginite has different tints of yellow, orange and brown colors. It is concentrated in the clayey matrix as thin laminae or flattened lenses (from 0.0*n* to *n* mm long) arranged parallel to bedding surfaces (Figs. 8c, 8e). The C_{org} content in the shales shows a positive correlation with the content and dimension of colloalginite aggregates.

One can observe in thin sections under great magnifications that the clayey matrix in carbonaceous shales contains a uniformly dissemination of the amorphous colloalginite-type OM. According to (Ginsburg, 1991), such aggregates of the clayey material (dominant component) and OM belong to "sorbomixtinite." The origin of sorbomixtinite in shales is evidently similar to that of colloalginite except for a slight compositional difference. Increase in the share of sorbomixtinite (relative to colloalginite) is particularly notable in the relatively low-carbonaceous (calcareous and clayey) shale varieties. For example, the relatively C_{org}-rich calcareous shales in members I and, partly, II are characterized by small colloalginite aggregates in the calcareous–clayey matrix. In such shales, the content of sorbomixtinite is comparable with that of colloalginite.

Shale varieties with the highest C_{org} contents from members II and, particularly, III include numerous large colloalginite aggregates. In contrast, they are insignificant in the OM of sorbomixtinite. Such OM is primarily confined to the foliated oil shales in the uppermost part of the shale-bearing sequence.

Carbonaceous shales always contain an admixture (5–10%) of small detritus of terrestrial OM represented by black to dark brown opaque angular fragments of plant tissues (inertinite). The size and abundance of plant remains increase notably in the upper part of the shale-bearing sequence and reach maximum values in shale varieties with the maximal silt contents.

High-carbonaceous shales contain an insignificant admixture (up to 1%) of sporomorph remains represented by cysts of dinoflagellates and spores and pollen of terrestrial plants.

In clayey–calcareous sediments, OM occurs usually in finely dispersed form (Fig. 8). The OM content shows negative correlation with CM. It is difficult to determine the origin (terrestrial or marine) of finely dispersed OM in these sediments. Colloalginite and sorbomixtinite occur as an admixture mainly in relicts of the primarily carbonaceous laminae destroyed by bioturbation. An admixture of finely dispersed plant detritus is present in clayey sediments. However, since other plant remains were not preserved or accumulated, precisely this OM becomes dominant and governs pyrolytic parameters to a significant extent.

Pyrolytic parameters of OM. Table 2 presents the results of pyrolytic studies of OM in samples of the most representative carbonaceous shales and clayey sediments from different parts of the section.

One can see that OM in sediments is generally characterized by low catagenetic maturity, which is evident from temperature values corresponding to the maximal extraction of hydrocarbon compounds during the heating of samples in an inert atmosphere ($T_{max} < 435$°C) (Tissot and Welte, 1978; Lopatin and Emets, 1987).

In some samples of clayey sediments with low C_{org} contents (upper half of the section, samples 20b and 29) T_{max} values are higher (up to 444 and 458°C, respectively), which may be explained by the occurrence of inertinite, i.e., detritus of substantially transformed OM redeposited from older sediments. The presence of inertinite increases usually T_{max} of OM in sedimentary rocks (Lopatin and Emets, 1987).

The OM generation potential, which is determined by the $(S_1 + S_2)$ value, corresponds to the total quantity of HC compounds released from OM during the heating of samples up to *S* and 300–600°C (S_2) S_1 characterizes the bitumen content in the rock, while S_2 characterizes the petroleum potential of kerogen at the moment of analysis (Tissot and Welte, 1978; Lopatin and Emets, 1987).

Table 2. Characteristic of OM from Volgian sediments of the Ivkino section based on petrographic and pyrolytic data

Member	Sample	Rock	OM dominant type	T_{max}, °C	S_1, mg HC/g rock	S_2, mg HC/g rock	TOC, % of rock	HI, mg HC/g TOC
I	4*a*	Carbonaceous shale, calcareous	Colloalginite, sorbomixtinite	409	0.99	53.78	11.74	458
	4*b*	Dark calcareous–clayey rock	Finely dispersed OM, small phytodetritus	425	0.04	2.88	2.45	117
	7*a*	Carbonaceous shale, calcareous	Colloalginite, sorbomixtinite	409	1.77	69.13	14.04	402
	7*c*	Light calcareous–clayey rock	Finely dispersed OM	424	0.03	1.76	1.83	96
	9*a*	Dark calcareous–clayey rock	Sorbomixtinite, colloalginite, small phytodetritus	419	0.08	8.63	3.68	234
	10*c*	Light calcareous–clayey rock	Finely dispersed	419	0.01	0.08	0.46	17
II	12*a*	High-carbonaceous shale	Colloalginite, sorbomixtinite, sporomorph complexes	399	3.55	184.6	26.74	690
	14*c*	Light calcareous–clayey rock	Finely dispersed OM, small phytodetritus	426	0.04	2.82	2.82	100
	20*b*	Dark calcareous–clayey rock	Finely dispersed OM, small phytodetritus	444	0.04	1.67	1.91	87
	21	Carbonaceous shale, clayey	Colloalginite, sorbomixtinite	414	4.26	74.29	16.5	450
	22	High-carbonaceous shale	Colloalginite	412	2.35	110.2	20.5	537
III	27*a*	Carbonaceous shale, silty	Sorbomixtinite, small phytodetritus, colloalginite	406	1.32	32.86	10.87	302
	28-*1*	High-carbonaceous shale	Colloalginite	410	3.27	146.1	26.17	558
	29	Dark calcareous–clayey rock	Small phytodetritus	458	0.07	0.4	1.78	22
	30-*1*	High-carbonaceous shale	Colloalginite	407	5.09	159.6	24.07	663

The generation potential of Volgian carbonaceous shales in the study area is high (32.86–159.6 HC/g), while the potential of clayey–calcareous rocks is low (0.40–2.82 HC/g).

The total organic carbon (TOC) parameter corresponds to the sum of pyrolyzed and residual organic carbon (%). The TOC and C_{org} values determined by different methods in samples taken from the same layers are similar for the OM-depleted clays and carbonaceous shales with the highest C_{org} concentrations. At the same time, the TOC and C_{org} values are sometimes different in shales with the relatively low OM contents, which may be explained by different potentialities of analytical methods and extremely irregular distribution of colloalginite in layers of these rocks.

The value of hydrogen index (HI = S_2/TOC) obtained for kerogen from carbonaceous shales varies from 402 to 690 mg HC/g TOC, which indicates its largely marine origin (Tissot and Welte, 1981). The highest HI values (537–690) are characteristic of carbonaceous shales with the maximal C_{org} concentrations in the upper half of the sequence (members II and III) enriched in colloalginite and subjected to minimal bioturbation. The maximal HI values are established for the high-carbonaceous foliated shale interbed from Member III (HI = 653, sample 30), which lacks fossils and bioturbation signs, and for sample 12 from Member II (HI = 690), where OM contains sporomorph components, in addition to the dominant colloalginite and the subordinate sorbomixtinite. The notably lower HI values are characteristic of calcareous and variably bioturbated clayey–silty shales, in which sorbomixtinite plays a notable role along with colloalginite.

Kerogen in Volgian shales belongs to types I and II originating largely from marine microplankton. The hydrocarbon part of primary OM is well preserved despite its oxidizing biochemical destruction.

Clayey–calcareous sediments are characterized by substantially lower HI values (17–302). Its minimal values (17–100) are typical for the colloalginite-free rocks (C_{org} <3%). The HI values are determined primarily by the occurrence of finely dispersed allochthonous plant detritus (inertinite). In clayey sediments with particles of altered colloalginite or small fragments composed of colloalginite and sorbomixtinite that survived bioturbation, the HI values increase up to 117–302.

Both carbonaceous shales and clayey–calcareous sediments demonstrate positive correlation between HI and C_{org} (TOC) concentrations (Fig. 7). They also show correlation between HI, colloalginite content, and low degree of bioturbation of primary sediments by burrowing organisms. In general, the available data indicate the dependence of HC preservation degree in OM on the quantity of its allochthonous marine component.

Sediments Overlying the Shale-Bearing Sequence

Sediments overlying the shale-bearing sequence with a sharp boundary are composed of sandy–silty material and clay admixture. The virtual lack of sedimentation bedding in them is evidently related to intense bioturbation (Fig. 8g). They are characterized by a high content of glauconite (Fig. 8h). Locally, glauconite serves as cement for terrigenous mineral grains, which implies the in situ formation of at least some part of glauconite.

DISTRIBUTION OF CHEMICAL ELEMENTS ACROSS THE SECTION

The distribution of many chemical elements was studied in lower Kimmeridgian, middle Volgian shale-bearing, and overlying sediments.

It is rather difficult to reveal the distribution of elements in alternating beds of geochemically contrasting sediments, because their geochemical signature could be formed at both sedimentary and postsedimentary (primarily, early diagenetic) stages. In the considered case, the influence of postdiagenetic processes on the redistribution of elements can be excluded, since the absence of any notable catagenetic transformations of this sequence is evident from specific features described above.

In order to estimate the influence of CM and OM contents on the distribution of elements, we used their Al-normalized concentrations (“element/Al coefficient”). Such an approach is frequently used in geochemical studies (Brumsack, 1989; Hild and Brumsack, 1998; Lipinski et al., 2003; Riboulleau et al., 2003; and others) and is based on close relations between Al and terrigenous constituent. The Al content in the latter component is largely determined by the mineral composition of rocks in provenances with the consideration of the inert behavior of Al during the diagenetic redistribution of elements in sediments. Comparison between normalized and primary data shows that elements during sedimentation and diagenesis behave in a similar way (Fig. 9).

The extremely irregular distribution of OM both across the entire sequence and separate sedimentary cyclites represents its main geochemical feature. Most elements respond to this type of OM distribution in specific ways.

Most significant variations in the OM content (0.98 to 1.59%) are characteristic of *lower Kimmeridgian* sediments (Table 1, Samples 1, 2). Despite low OM contents, concentrations of elements, such as Ni, Co, Cu, Zn, Mo, Ag, and As, in some samples exceed notably their average values characteristic of clayey sediments (Turekian and Wedepohl, 1961; Vinogradov, 1962; Wedepohl, 1991). Some samples demonstrate elevated Mn and P contents (Table 1, sample 2). It should be noted that the Ni, Co, and Zn contents are increased to a lesser extent in the lower part of the member.

High concentrations of these elements can be related to the influence of some provenances at the sed-

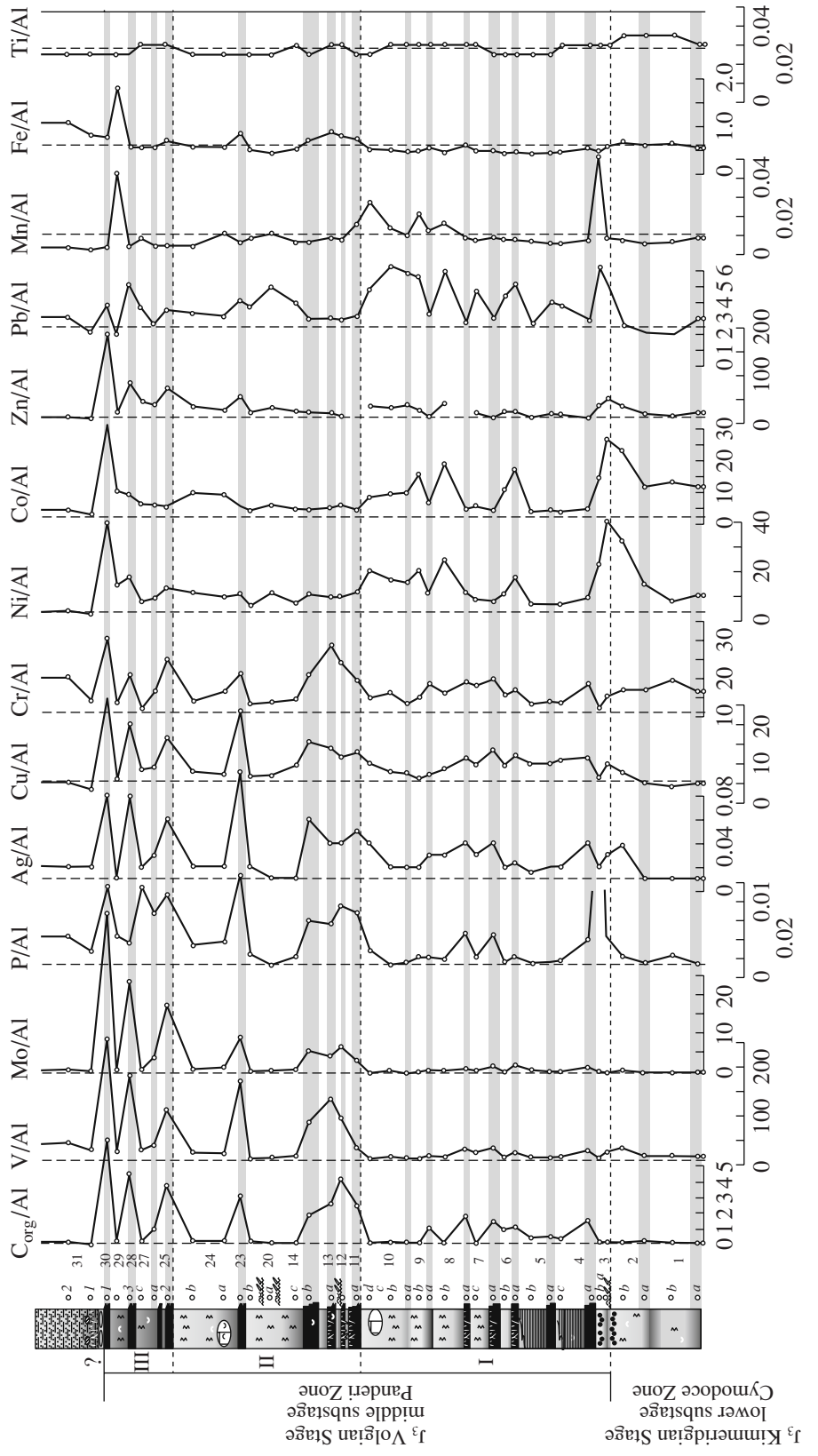

Fig. 9. Al-normalized distribution of chemical elements in the Ivkino section. Vertical dashed line shows el/Al values calculated as ratio between average contents of a specific element and Al (8.0%) in clayey rocks, after (Turekian and Wedepohl, 1961; Wedepohl, 1991). For lithological legend, see Fig. 2.

imentation stage, but no reliable evidence for the existence of such provenances is available.

Increase in contents of these elements in the uppermost lower Kimmeridgian sediments is most likely related to their redistribution during diagenesis. Termination of the accumulation of Kimmeridgian sediments due to regression could promote the exhumation of recently accumulated sediments, in which diagenetic transformations were in progress. Development of reducing conditions in bottom sediments is evident from the abundance of small pyrite aggregates. Due to drying of bottom sediments, interstitial waters with dissolved compounds of different elements began to migrate intensely toward the surface and evaporate, resulting in the precipitation of elements.

High concentrations of approximately the same elements are also observed in a thin (no more than 0.2 m) bed of calcareous clays at the base of the shale-bearing sequence. They were likely accumulated at the initial stage of the middle Volgian transgression due to the partial erosion of underlying sediments with high concentrations of these elements; i.e., enrichment with some chemical elements was most likely an inherited process.

In the *shale-bearing sequence*, the distribution of elements was controlled by factors that were active at both sedimentation and diagenesis stages accompanied by the redistribution of elements within sediments. It is most probable, however, that these factors acted simultaneously and their contribution to the final distribution pattern of elements was different.

Some elements correlate distinctly with OM, high concentrations of which in the carbonaceous shales appeared at the sedimentation stage. Correlation between OM and V is traced well from the parallel increase in contents of these components upward the section and within separate cycles: high V contents are noted in the carbonaceous shales at the base of cycles, while relatively low V concentrations are characteristic of clayey sediments. As follows from Table 1 and Fig. 9, concentrations of V in shales from the upper part of the section are very high (1000–1200 ppm), which exceeds 8–10 times its background values. Mn shows a similar behavior: its concentration in shales from some parts of members II and III is 1.0–1.5 orders of magnitude higher than the background value. Similar or close behavior is also noted for P, As, and, locally, Cu and Cr.

The main process responsible for high concentrations of elements in the shales was likely to be their sorption on the surface of OM particles at the sedimentation stage. Diffusion of elements from bottom waters into carbonaceous sediments could also contribute to the concentration of elements.

The distribution of Ni and geochemically related elements across the sequence is characterized by different patterns. Table 1 and Figure 9 show that the Ni content in clayey sediments in sedimentary cycles of members I and II is locally higher than in the underlying carbonaceous shales. However, high Ni concentrations are observed in carbonaceous shales rather than clays in rocks of Member III.

Such distribution pattern of Ni could result from its diagenetic redistribution in sediments. Lithologically contrasting cyclites with high and extremely low OM contents in carbonaceous and clayey–calcareous sediments, respectively, were accumulated in substantially different redox environments: sharply reducing conditions in the carbonaceous sediments and slightly reducing (sometimes, probably oxidizing) environment in the clayey-calcareous sediments. Correspondingly, Ni in carbonaceous sediments was transformed into labile forms, which diffused into the adjacent clayey–calcareous sediments and precipitated under different Eh conditions. Moreover, Ni could migrate into both overlying and underlying strata. At the sedimentation stage, carbonaceous sediments were evidently characterized by higher Ni contents, and the present-day distribution of Ni is related to its redistribution between the adjacent layers during diagenesis. This inference is supported by the Ni distribution in sediments of Member III characterized by the maximal OM concentration. At the same time, notable C_{org} concentrations are also recorded in the clayey sediments alternating with the shales. Hence, both types of sediments were characterized by well-developed reducing conditions during diagenesis. Correspondingly, no significant Eh gradient existed between these sediments. Hence, the environment did not foster intense redistribution of elements and their diffusion from the carbonaceous shales into the clayey sediments.

Based on the behavior in geochemically contrasting layers, Co, Zn, Mn, and, to a lesser extent, Pb belong to the Ni group. The low-contrast distribution of elements across the sequence, as well as slightly increased contents of B, Ga, and Ge in the clayey sediments, are most likely related to their association with the clayey matter.

Distribution of Fe lacks any correlation with particular parts of sedimentary cyclites. Its general distribution across the section demonstrates a decreasing trend in sediments of Member I and slight increasing trend in members II and III. This statement is also valid for Cr and Sn.

It should be noted that behavior of chemical elements in the Kimmeridgian and Volgian sediments was also certainly affected by bioturbation that mixed the sediments, changed their permeability, and influenced diagenetic processes. However, issue of the influence of bioturbation on the geochemistry of sediments requires special consideration.

The shale formation stage was followed by the accumulation of sandy–silty sediments that differ substantially from the underlying strata in terms of geochemistry: moderate concentrations of OM (C_{org} ~1%) and clarke-level contents of most elements. High Fe contents (6.9–7.4%) in these sediments are rather typical of basal layers of the sequence accumulated in the course of transgression. Since iron hydroxides are good sorbents, it seems quite natural that V concentrations in

these sediments are also high: geochemical behavior of these elements during sedimentation is often similar (Kholodov, 1973 and others). A significant share of Fe in these sediments was incorporated into glauconite during diagenetic transformations.

DISCUSSION

The study of the Ivkino section reveals that its shale-bearing sequence is more complete than other coeval successions in the Middle Volga region: rarer traces of erosion, condensation, and softgrounds. At the same time, the Ivkino section lacks the sandstone horizon and "phosphorite plate" developed at the top of the Volgian sequence in the Gorodishche section. This can be related to the following reasons: (1) subsequent erosion of the upper part of the section; (2) greater distance from the bank; and (3) existence of geomorphological barriers for the progradation of sandy fractions. The Middle Volga region could also accumulate the pain portion of sandy material transported by rivers from the west. The greater completeness of the shale-bearing sequence could be related to its accumulation either in deeper settings (there is no direct evidence for this assumption except the lesser content of littoral benthic fauna in sediments) or in hydrodynamically calm settings of the paleobasin probably surrounded by morphological barriers.

Analysis of fossils in lithologically different sediments of the Ivkino section shows that ecology in the paleobasin was extremely unstable during accumulation of the shale-bearing sequence. Clayey–calcareous sediments with low OM contents were accumulated in environments favorable for different organisms typical of normally aerated basins. In contrast, their habitat conditions was sharply deteriorated during the deposition of organic-rich sediments, resulting in the abundance of juvenile molluscan shells in carbonaceous shales and the drastic reduction of nannoplankton and other benthic and planktonic remains.

Significant outburst in bioproductivity of organic-walled plankton (planktonic bacteria, various species of microalgae, and others) could foster the development of different factors unfavorable for the biota. For example, accumulation of high-carbonaceous sediments could stimulate the development of anoxic conditions in the water column. This is evident from finds in other sections (Bushnev, 2007) of isorenierathene derivatives—biomarkers of the photosynthesizing alga of the genus *Chlorobium* that dwelt in the photic zone at the boundary with the H_2S-contaminated watermass (Damste et al., 1993, 1995; Repeta and Simpson, 1991; Repeta et al., 1989; and others). At the same time, anoxic conditions in the shallow basin could hardly be stable and should include a relatively thick bottom water layer. Another negative factor could be represented by extremely high intensity of organic-walled plankton bloom, which consumed the main portion of biophile elements and restricted the development of other microbiotic forms, carbonate-producing organisms included. As was shown above, sharp increase in the OM content was accompanied by a significant decrease in the content of the carbonate component in sediments (Fig. 7). Finally, we should not also rule out an additional aspect of this bloom (red tides). Observations in present-day seas have revealed that the red tides can often be toxic and they can affect negatively most macro- and microbiotic organisms. Thus, intense bloom of organic-walled plankton could provoke sharp deterioration of paleoecological conditions in both bottom and surface waters of the Volgian sea (Gavrilov and Kopaevich, 1996). Moreover, ecological conditions could fluctuate during the accumulation of carbonaceous sediments, which is evident from finds of benthic organisms (although distinctly suppressed) at bedding surfaces.

It should also be kept in mind that abundance of both macro- and microfossils decreases upward the section up to their complete disappearance, which is evident from the distribution of ammonites and nannofossils. We should note a brief episode of ecological setting normalization at the level of Bed 24, as suggested by the episodic appearance of these fossils.

What is the factor responsible for significant fluctuations in paleoecological settings and their general deterioration trend toward the late accumulation stage of Volgian sediments? The answer to this question may be obtained after considering dynamics of the shale-bearing sequence formation.

Like in sections of the Middle Volga region, the structure of the Upper Jurassic sequence in the Ivkino section implies that the general (mainly regressive) development trend of the late Kimmeridgian basin was complicated by regression–transgression cycles of at least three orders. Among them, two regression episodes (prior to and after the accumulation of the shale-bearing sequence) are most distinct. Both these episodes are reflected in the section as sharp changes in sedimentation settings, which produced lithologically and geochemically different sediments.

Two other regression episodes occurred during the formation of the shale-bearing sequence. They divided the single stage of its deposition into three substages corresponding to accumulation of members I, II, and III. Member I is crowned by a bed of carbonate concretions. Their appearance is evidently related to a relatively slight erosion of the condensed bed with the high content of reworked biogenic CM, which was redistributed during diagenesis and transformed into concretions. Such beds frequently mark the roofs of sedimentary cycles at the end of regressive episodes.

The smallest elements of the section related to sea-level fluctuations are represented by sedimentary cyclites mentioned above that are identified in both Kimmeridgian and Volgian sediments with specific features at different stratigraphic levels. They are most likely governed by Milankovitch cycles. Sharp contacts of shales with the underlying sediments and, in con-

trast, their gradual transitions to the overlying elements of cyclites suggest that their formation began with transgressions and terminated with sealevel fall and insignificant erosion of accumulated sediments (at the roof of cyclites). The amplitude of sealevel fluctuations probably did not exceed a few meters.

Based on finds of chlorophyll in the OM of shales, Strakhov (1934, 1962) explained episodes of intense accumulations of organic-rich sediments by the formation of "underwater meadows" in the basin with the development of phytobenthos. Cyclicity of these events was attributed to presumably tectonic movements of seafloor and its intermittent exhumation to the photic zone.

In our opinion, the formation mechanism of the shale-bearing sequence was slightly different. First, we should elucidate why the initial stage of cyclite formation was marked by the accumulation of carbonaceous sediments that gave way to the clayey–calcareous sediments. The pulsating character of carbonaceous sediment accumulation can best be explained by the model previously proposed for the formation of organic-rich sediments during rapid and relatively brief transgressions (Gavrilov, 1994; Gavrilov et al., 1997, 2002, 2003, 2004). Its essence consists in the following. Areas released from seawater during the humid climate at the regression stage were marked by the rapid formation of soils and lacustrine–boggy landscapes that were favorable for the accumulation of both solid and dissolved forms of OM and compounds of biophile elements, such as P, N, Fe, and others. When the regression gave way to the next transgressive stage, seawaters interacted with the landscapes and released biophile elements, resulting in the outburst in bioproductivity of planktonic bacteria, organic-walled dinoflagellates, and other low-organized biotic forms (correspondingly, in the accumulation of organic-rich sediments). At the same time, solid plant OM released from the landscapes also participated in the formation of carbonaceous sediments. This assumption is supported by the pyrolytic analysis of OM indicating its mixed composition: dominant aqueous and subordinate continental materials. At the initial transgression stages, biophile elements were mainly provided by terrestrial coastal landscapes. Beginning of the accumulation of organic-rich sediments triggered the recycling of biophile elements in the sedimentation basin itself, i.e., return of some elements (primarily, phosphorus) from the reduced sediments. Recycling could maintain high bioproductivity in the basin even under conditions of decelerated transgression characterized by decrease in the influx of biophile elements. Inference on recycling is confirmed by the data on the distribution of phosphorus in the shaly sequence. As was mentioned above, we can see a positive correlation between C_{org} and P. However, if the entire phosphorus transported with OM had been buried in the sediments, the present-day phosphorus concentrations in shales should be significantly higher. When the transgression ceased and the recycling attenuated, the formation of carbonaceous shales was replaced by the accumulation of background clayey–calcareous sediments. Fluctuation of bioproductivity could also be affected by an additional factor. The cyclic sealevel fall in the basin and its shoaling at this stage could provide conditions for greater heating of the water column phytoplankton development.

Thus, different microplankton groups dominated at different formation stages of sedimentary cycles: organic-walled organisms dominated at the initial stage, whereas the carbonate-producing organisms (nannoplankton, foraminifers, and others) prevailed at the later stages. Multiple changes in biogenic sedimentation produced the cyclic shale-bearing sequence.

It should be noted that accumulation of upper elements of cyclites (clayey–calcareous sediments) was accompanied by the influx of OM from different sources. However, OM buried together with the calcareous microplankton was unstable and almost completely decomposed in the course of diagenetic processes. In contrast, the relatively small amount of terrestrial OM transported to the basin at this stage was already oxidized to a significant extent. Hence, the OM was inert and buried in sediments without substantial losses. Therefore, hydrogen index in clayey–calcareous sediments was very low (Table 2).

Appearance of the Volgian high-carbonaceous rocks, which differ substantially in terms of lithological–geochemical parameters from other Jurassic sediments of the East European Platform, poses the question concerning factors responsible for the sharp increase in OM accumulation rate at the particular stage of basin development. The formation mechanism of sedimentary cycles (OM concentration in the lower parts) also functioned before the accumulation of shales: cyclicity is observable in the entire Upper Jurassic section of the East European Platform. During the high stable stand of sea level, however, influence of its low-amplitude fluctuations influenced on the influx of biophile elements from coastal landscapes was insignificant, resulting in a weak compositional difference between the lower and upper elements of the cycle.

The paleogeographic situation changed notably after the hiatus related to the sealevel fall in the terminal Kimmeridgian time. Although the Volgian transgression was rapid and powerful, amplitude of the sealevel rise was substantially lower than that in the Kimmeridgian time. This feature promoted the following processes. First, a wide coastal zone with the development of soils and lacustrine–boggy landscapes was formed. Second, intrabasin uplifts turned into islands (archipelagoes) with landscapes similar to those on the main land were exposed. The relief in these landscapes was flat, because it was previously smoothed away by marine erosion and sedimentation. Correspondingly, even low-amplitude sealevel fluctuations (in particular, rises) resulted in the flooding of spacious lowlands, intense influx of biophile elements, rapid growth of bioproductivity of the organic-walled microbiota, and accumulation of high-carbonaceous sediments.

Such processes were in progress during the Panderi phase of the middle Volgian Age. The accumulation period of shale-bearing sequence was marked by two high sealevel falls, in addition to its low-amplitude fluctuations responsible for the formation of elementary cycles. The subsequent sealevel fluctuations were characterized by the attenuating patterns: each subsequent sealevel rise was always lower than the previous one. Consequently, sediments of each of the three successive members were accumulated in progressively shallower environments. It should also be noted that the close spacing of carbonaceous beds at the base of Member II (as well as in the reduced Member III) is related to their accumulation in relatively shallow-water settings in the course of transgression. The transgression peak and sealevel stabilization were followed by the accumulation of thicker cyclites with well-developed lower, middle, and upper elements.

Such a sedimentation scenario in the Late Jurassic also explains some geochemical features of the shale-bearing sequence. In particular, the upsection increase in the OM content becomes clear, because bioproductivity of the basin was maximal near sources of biophile elements (land areas) and the basin was gradually shoaling. Since land provided the majority of chemical elements, their maximal concentrations are also confined to the coastal zone of maximal bioproductivity. The coastal zone served as a peculiar biofilter that entrapped a wide range of elements. Since the elements were delivered from both land and newly formed islands, the basin hosted many zones of elevated bioproductivity at this stage. Around relatively high uplifts turned into islands prior to other areas, carbonaceous sediments could also begin to accumulate earlier than in other areas of the basin where islands appeared later. It is rather difficult to correlate the sections because of the patchy distribution of facies related to the intricate relationships described above. Thus, different-order sealevel fluctuations represented a powerful regulator of sedimentation dynamics and geochemical properties of sediments.

Comparison of the Ivkino and Gorodishche (Middle Volga region) sections reveals their structural similarity: each section comprises three members, which are characterized, in turn, by similar internal structures in different sections. Such a structural similarity of sections located almost 400 km away from each other indicates that they reflect similar trends in the development of the middle Volgian basin in the Russian Plate.

CONCLUSIONS

Analysis of lithological–geochemical properties of Volgian sediments in the Ivkino section and its macro- and micropaleontological characteristics allows the following inferences.

(1) The shale-bearing sequence is characterized by a distinct cyclic structure. Elementary sedimentary cyclites consist of three elements: lower bed carbonaceous shales, middle bed of dark gray clayey–calcareous sediments, and upper bed of light gray clayey–calcareous sediments. Transitions between the elements of cyclites are gradual, whereas transitions between individual cyclites are sharp.

(2) The pyrolytic and microscopic studies demonstrate the prevalence of basinal OM in shales (kerogen of types I and II, C_{org} content up to 20% or more). The subordinate terrestrial OM (kerogen of type III) occurs usually in the slightly organic-rich clayey–calcareous sediments.

(3) The shale-bearing sequence is composed of geochemically contrasting sediments: concentrations of many elements in carbonaceous beds are one to two orders of magnitude higher than their background values in some places. Their contents are low in the clayey–calcareous sediments. The distribution of elements across the section was determined by factors that acted at both sedimentation and diagenesis stages.

(4) Lithological characteristics in different intervals of the Jurassic section imply that sediments were accumulated in progressively shoaling settings in the following succession: lower Kimmeridgian, middle Volgian, and overlying sequence. Sedimentation settings were also characterized by the shoaling trend during the accumulation of the shale-bearing sequence.

(5) The ammonite and nannofossil assemblages indicate unfavorable habitat conditions in the basin during the accumulation of carbonaceous sediments.

(6) The shale-bearing sequence was accumulated in the course of frequent short-period sealevel fluctuations. During transgressions, onshore landscapes provided the influx of biophile elements into the basin, which triggered the outburst in productivity of organic-walled phytoplankton and stimulated the accumulation of carbonaceous sediments. Recycling of biophile elements also enhanced high productivity.

(7) The structure of the shale-bearing sequence in the Ivkino section is similar to the structure of coeval sections in the Middle Volga region. This fact reflects general regularities in development of the middle Volgian basin of the Russian Plate.

ACKNOWLEDGMENTS

This work was supported by the Russian Foundation for Basic Research (project nos. 06-05-65282 and 06-05-64284) and Foundation of the President of the Russian Federation (project no. MK-3235).

REFERENCES

Baraboshkin, E.Yu., Veimarn, A.B., Kopaevich, L.F., and Naidin, D.P., *Izuchenie stratigraficheskikh pereryvov pri proizvodstve geologicheskoi s"emki* (Studies of Stratigraphic Hiatuses during Geological Mapping), Moscow: Mosk. Gos. Univ., 2002.

Bornemann, A., Aschwer, U., and Mutterlose, J., The Impact of Calcareous Nannofossils on the Pelagic Carbonate Accumulation across the Jurassic–Cretaceous Boundary, *Palaeo-*

geogr., Palaeoclimatol., Palaeoecol, 2003, vol. 199, pp. 187–228.

Bown, P.R., Cooper, M.K.E., and Lord, A.R., A Calcareous Nannofossil Biozonation Scheme for the Early to Mid Mesozoic, *Newslett. Stratigr.*, 1988, vol. 20, pp. 91–114.

Bralower, T.J., Monechi, S., and Thierstein, H.R., Calcareous Nannofossil Zonation of the Jurassic-Cretaceous Boundary Interval and Correlation with the Geomagnetic Polarity Timescale, *Mar. Micropaleontol.*, 1989, vol. 14, pp. 153–235.

Bromley, R.G., *Trace Fossils. Biology, Taphonomy and Applications (Second Edition)*, London: Chapman and Hall, 1996.

Brumsack, H.-J., Geochemistry of Recent TOC-Rich Sediments from the Gulf of California and Black Sea, *Geol. Rundshau*, 1989, vol. 78, no. 3, pp. 851–882.

Bushnev, D.A., Geochemistry of Organic Matter in Carbonaceous Sequences of the East European Platform, *DSc (Geol.-Miner.) Dissertation*, Syktyvkar: Inst. Geochim. Kolsk. Nauchn. Tsentra Ural. Otd. Ross. Akad. Nauk, 2007.

Damste, J.S.S., Koster, J., Baas, M., et al., Cyclisation and Aromatisation of Carotenoids during Sediment Diagenesis, *J. Chem. Soc. Chem. Commun.,* 1995, no. 2, pp. 187–188.

Damste, J.S.S., Wakehan, S.G., and Kohnen, M.E.L., et. al., A 6000-Year Sedimentary Molecular Record of Chemocline Excursions in the Black Sea, *Nature*, 1993, vol. 362, pp. 827–829.

Dobryanskii, A.F., *Goryuchie slantsy SSSR* (Oil Shales of the USSR), Leningrad, Moscow: Gostoptekhizdat, 1947.

Gavrilov, Yu.O., Possible Causes of Accumulation of OrganicñRich Deposits in Terms of Eustatic Oscillations of the Sea Level, in *Ekosistemnye perestroiki i evolyutsiya biosfery* (Ecosystem Transformations and Biospheric Evolution), Rozanov, A.Yu. and Semikhatov, M.A., Eds., Moscow: Nedra, 1994, pp. 305–311.

Gavrilov, Yu.O. and Kopaevich, L.F., Geochemical, Biochemical, and Biotic Consequences of Eustatic Oscillations, *Stratigr. Geol. Korrelyatsiya*, 1996, vol. 4, no. 4, pp. 3–14 [*Stratigr. Geol. Correlation* (Engl. Transl.), 1996, vol. 4, no. 4, pp. 315–325].

Gavrilov, Yu.O. and Shcherbinina, E.A., Global Biosphere Event at the Paleocene–Eocene Boundary, in *Sovremennye problemy geologii* (Modern Problems of Geology), Gavrilov, Yu.O. and Khutorskoy, M.D., Eds., Moscow: Nauka, 2004, pp. 493–531.

Gavrilov, Yu.O., Shcherbinina, E.A., and Oberhänsli, H., Paleocene/Eocene Boundary Events in the Northeastern Peri-Tethys, in *Causes and Consequences of Globally Warm Climates in the Early Paleogene*, Wing, S.L., Gingerich, P.D., Schmitz, B, and Thomas, E. Boulder, Eds., Colorado: Geol. Soc. Am. Spec. Paper 369, 2002, pp. 147–168.

Gavrilov, Yu.O., Kodina, L.A., Lubchenko, I.Yu., and Muzylev, N.G., The Late Paleocene Anoxic Event in Epicontinental Seas of Peri-Tethys and Formation of the Sapropelite Unit: Sedimentology and Geochemistry, *Litol. Polezn. Iskop.,* 1997, vol. 32, no. 5, pp. 492–517 [*Lithol. Mineral. Res.* (Engl. Transl.), 1997, vol. 32, no. 5, pp. 427–450].

Gavrilov, Yu.O., Shchepetova, E.V., Baraboshkin, E.Yu., and Shcherbinina, E.A., The Early Cretaceous Anoxic Basin of the Russian Plate: Sedimentology and Geochemistry, *Litol. Polezn., Iskop.*, 2002, vol. 37, no. 4, pp. 359–380 [*Lithol. Mineral. Res.* (Engl. Transl.) 2002, vol. 37, no. 4, pp. 310–329].

Gerasimov, P.A. and Mikhailov, N.P., The Volgian Stage and Unified Stratigraphic Scale of the Upper Stage of the Jurassic System, *Izv. Akad. Nauk SSSR, Ser. Geol.*, 1966, no. 2, pp. 118–138.

Gerasimov, P.A., Migacheva, E.E., Naidin, D.P., and Sterlin, B.L., *Yurskie i melovye otlozheniya Russkoi platformy* (Jurassic and Cretaceous Deposits in the Russian Platform), Moscow: Mosk. Gos. Univ., 1962.

Ginzburg, A.I., *Atlas petrograficheskikh tipov goryuchikh slantsev* (Atlas of Petrographic Types of Oil Shales), Leningrad: Nedra, 1991.

Giraud, F., Pittet, B., Mattioli, E., and Audouin, V., Paleoenvironment Controls on the Morphology and Abundance of the Coccolith Watznaueria Britannica (Late Jurassic, Southern Germany), *Mar. Micropalaeontol.,* 2006, vol. 60, no. 3, pp. 205–225.

Hild, E. and Brumsack, H.-J., Major and Minor Element Geochemistry of Lower Aptian Sediments from NW Germany Basin (Core Hoheneggelsen KP40), *Cretaceous Res.*, 1998, vol. 19, pp. 625–633.

Ilovaiskii, D.I. and Florenskii, K.P., Upper Jurassic Ammonites in Basins of the Ural and the Ileka Rivers, in *Materialy k poznaniyu geologicheskogo stroeniya SSSR. Novaya Seriya* (Materials on Geological Structure of the USSR. New Series), 1941., no. 1, pp. 7–195.

Ivanov, A.P., Geological Description of Phosphorite-Bearing Deposits in the Kostroma Province in the Volga River East of Kineshma and in the Unzha and the Neya Rivers, in *Otchet po geologicheskomu issledovaniyu fosforitovykh zalezhei. Trudy komissii Moskovskogo sel'skokhozyaistvennogo instituta po issledovaniyu fosforitov* (Report on Geological Study of Phosphorite Deposits: Transacts of Commission of the Moscow Agricultural Institute on the Study of Phosphorites), Samoilov, Ya., Ed., Kostroma Province, 1909, no. 1, pp. 71–145.

Kessels, K., Mutterlose, J., and Ruffell, A., Calcareous Nannofossils from Late Jurassic Sediments of the Volgian Basin (Russian Platform): Evidence for Productivity-Controlled Black Shale Deposition, *Int. J. Earth Sci.*, 2003, vol. 92, no. 5, pp. 743–757.

Kholodov, V.L., *Osadochnyi rudogenez i metallogeniya vanadiya* (Sedimentary Ore genesis and Metallogeny of Vanadium), Moscow: Nauka, 1973.

Khudyaev, I.E., *Mezozoiskie osadki v raione r. Sysoly (po kollektsiyam L.I. Lutugina*) (Mesozoic Sediments in the Sysola River Region. Based on Collections of L.I. Lutugin), Leningrad: Izv. Geol. Komit., 1927, vol. 46, no. 5, pp. 497–522.

Krotov, P., Data on Geology of the Vyatka Province: Communication 3. Geological Study of Northern Zone of the Vyatka Province, *Tr. O-va Estestvoispyt. Kazan. Univ.,* 1879, vol. 8, no. 2.

Kutek, J., The Scythicus Zone (Middle Volgian) in Poland: Its Ammonites and Biostratigraphic Subdivisions, *Acta Geol. Polon.*, 1994, vol. 44, nos. 1–2, pp. 1–33.

Lipinski, M., Warning, B., Brumsack, H.-J., Trace Metals Signatures of Jurassic/Cretaceous Black Shales from the Norwegian Shelf and the Barents Sea, *Palaeogeogr., Palaeoclimatol., Palaeoecol.*, 2003, vol. 190, pp. 459–475.

Lopatin, N.V. and Emets, T.P., *Piroliz v neftegazovoi geokhimii* (Pyrolysis in Petroleum Geochemistry), Moscow: Nauka, 1987.

Lord, A.R., Cooper, M.K.E., Corbett, P.W.M., et al., Microbiostratigraphy of the Volgian Stage (Upper Jurassic), Volga River, USSR, *Neues Jahrb. Geol. Palaontol. Monatsh.*, 1987, vol. 10, pp. 577–603.

Lyyurov, S.V., *Yurskie otlozheniya severa Russkoi plity* (Jurassic Deposits of the Northern Russian Plate), Yekaterinburg: Ural. Otd. Ross. Akad. Nauk, 1996.

Mikhailov, N.P., Zonal Subdivision of the Lower Volgian Stage and Its Equivalents, in *Doklady sovetskikh geologov k I-mu Mezhdunarodnomu kollokviumu po yurskoi sisteme* (Reports of Soviet Geologists at I Int. Colloquium on the Jurassic System), Tbilisi: Akad. Nauk. Gruz. SSR, 1962, pp. 185–199.

Mikulash, R. and Dronov, A., *Paleoikhnologiya—vvedenie v izuchenie sledov iskopaemykh organizmov* (Paleoichnology: Introduction to the Study of Fossil Organism Traces), Prague: Geol. Inst. Acad. Sci. Czech Republic, 2006.

Mitta, V.V. and Starodubtseva, I.A., Field Work in 1998 and Biostratigraphy of the Lower Callovian of the Russian Platform, *VM-Novitates. Novosti Geol. Muzeya Ross. Akad. Nauk V.I. Vernadskogo*, 1998, no. 2.

Olfer'ev, A.G., Jurassic Stratigraphy in the Moscow Syneclise, in *Yurskie otlozheniya Russkoi platformy* (Jurassic Deposits in the Russian Platform), Leningrad: Vses. Nauchno-Issled. Geol. Razved. Inst., 1986, pp. 48–61.

Pimenov, M.V., Guzhikov, A.Yu., and Rogov, M.A., Preliminary Data on Magnetostratigraphic Study of the Upper Kimmeridgian Substage–Volgian Stage (Gorodishche Settlement, Ul'yanovsk District), Abstracts of Papers, *Materialy pervogo Vserossiiskogo soveshchaniya "Yurskaya sistema Rossii: problemy stratigrafii i paleogeografii"* (Proc. I All-Russia Conference "Jurassic System of Russia: Problems of Stratigraphy and Paleogeography"), Zakharov, V.A, Rogov, M.A., and Dzyuba, O.S., Eds., Moscow: Geol. Inst. Ross. Akad. Nauk, 2005, pp. 191–192.

Prognoz goryuchikh slantsev Evropeiskoi chasti SSSR (Prognosis of Oil Shales in the European Part of the USSR), Kotlukov, V.A. and Baukov, S.S., Ed., Tallin: Akad. Nauk Eston. SSR, 1974.

Repeta, D.J. and Simpson, D.J., The Distribution and Recycling of Chlorophyll, Bacteriochlorophyll and Carotenoids in the Black Sea, *Deep-Sea Res.*, 1991, vol. 38, Suppl. 2, pp. 969–984.

Repeta, D.J., Simpson, D.J., Jorgensen, B.B., et al., Evidence for Anoxygenic Photosynthesis from the Distribution of Bacteriochlorophylls in the Black Sea, *Nature*, 1989, vol. 342, pp. 69–72.

Repin, Yu.S., Zakharov, V.A., Meledina, S.V., and Nal'nyaeva, T.L., *Atlas mollyuskov Pechorskoi yury* (Atlas of Jurassic Mollusks in the Pechora), St. Petersburg: Nedra, 2006.

Riboulleau, A., Baudin, F., Deconink, J.-F., et al., Depositional Conditions and Organic Matter Preservation Pathways in an Epicontinental Environment: The Upper Jurassic Kashpir Oil Shales (Volgian Basin, Russia), *Palaeogeogr., Palaeoclimatol., Palaeoecol.,* 2003, vol. 197, pp. 171–197.

Rogov, M.A., Late Jurassic Mollusk Associations of the East European Platform, in *Biosfera–ekosistemy–bioty v proshlom Zemli: paleobiogeograficheskie aspekty,* (Biosphere–Ecosystems–Biota in the Earth's Past: Paleobigeographic Aspects), Gladenkov, Yu.B. and Kuznetsova, K.I., Eds., Moscow: Nauka, 2005, pp. 178–199.

Rogov, M.A., The Russian Platform as a Key Region for Volgian/Tithonian Correlation: A Review of the Mediterranean Faunal Elements and Ammonite Biostratigraphy of the Volgian Stage, *Rivista Ital. Paleontol. Stratigr.*, 2004, vol. 110, no. 1, pp. 321–328.

Rozanov, A.N., Portland Zones in the Moscow District and Probable Origin of the Portland Phosphorite Beds in the Moscow District, in *Materialy k Poznaniyu Geologicheskogo Stroeniya Rossiiskoi Imperii,* (Materials on Geological Structure of the Russian Empire), 1913, no. 4, pp. 17–103.

Rozanov, A.N., Zonal Classification of Rocks of the Lower Volgian Stage in the Simbirsk Province, *Izv. Mosk. Otd. Geol. Komiteta*, 1919 (1923), vol. 1, pp. 193–204.

Ruffell, A.H., Price, G.D., Mutterlose, J. et al., Late Jurassic Climate Change in the Volgian Basin (SE Russia): Clay Mineral and Calcareous Nannofossil Evidence, *Geol. J.*, 2002, vol. 37, pp. 17–33.

Shchepetova, E.V., Sedimentational and Geochemical Environments for the Formation of the Volgian Fuel Shales *Dorsoplanites Panderi* Sequence in the Northwestern Part of the Moscow Syneclise, in *Materialy pervogo Vserossiiskogo soveshchaniya "Yurskaya sistema Rossii: problemy stratigrafii i paleogeografii"* (Proc. I All-Russia Conference "Jurassic System of Russia: Stratigraphy and Paleogeography"), Zakharov, V.A., Rogov, M.A., and Dzyuba, O.S., Eds., Moscow: Geol. Inst. Ross. Akad. Nauk, 2005, pp. 256–261.

Shimkyavichus, P., Upper Jurassic Lithology and Clay Mineralogy in the Central Part of the East European Platform, in *Yurskie otlozheniya Russkoi platformy* (Jurassic Deposits of the Russian Platform), Leningrad: Vses. Nauchno-Issled. Geol. Razved. Inst., 1986, pp. 180–192.

Strakhov, N.M., *Osnovy teorii litogeneza* (Fundamentals of the Theory of Lithogenesis), Moscow: Akad. Nauk SSSR, 1962, vol. 2.

Strakhov, N.M., Oil Shales in the *Perisphinctes Panderi d'Orb Zone* (Essay on Lithology), *Byull. Mosk. O-va Ispyt. Prir., Otd. Geol.*, 1934, vol. 12, no. 2, pp. 200–248.

Thierry, J., Early Tithonian (141–139 My), in *Atlas Peri-Tethys, Palaeogeographical Maps,* Dercourt, J., et al., Eds., Paris: CCGM/CGMW, 2000, pp. 99–110.

Tissot, B. and Welte, D., *Petroleum Formation and Occurrence,* Heidelberg: Springer, 1979. Translated under the title *Obrazovanie I rasprostranenie nefti*, Moscow: Mir, 1981.

Tremolada, F., Bornemann, A., and Bralower, T.J., et al., Paleoceanographic Changes across the Jurassic/Cretaceous Boundary: The Calcareous Nannoplankton Response, *Earth Planet. Sci. Lett.*, 2006, vol. 241, pp. 361–371.

Turekian, K.K. and Wedepohl, K.H., Distribution of Elements in Some Major Units of the Earth's Crust, *Bull. Geol. Soc. Am.*, 1961, vol. 72, no. 2, pp. 175–192.

Vinogradov, A.P., Average Contents of Chemical Elements in the Main Types of Igneous Rocks in the Earth's Crust, *Geokhimiya*, 1962, no. 7, pp. 555–571.

Vishnevskaya, V.S., De Wewer, P., Baraboshkin, E.Yu., et al., New Stratigraphic and Paleo-Geographic Data on Upper Jurassic and Cretaceous Deposits from the Eastern Periphery of the Russian Platform, *Geodiversitas*, 1999, vol. 21, no. 3, pp. 347–363.

Wedepohl, K.H., The Composition of the Upper Earth Crust and Natural Cycles of Selected Metals, in *Metals and Their Compounds in the Environment*, Merian, E., et al., Eds., Weiheim: VCH-Verlagsgesellscaft, 1991, pp. 3–17.

Yavkhuta, G.V., The Upper Jurassic Shale-Bearing Formation (Volga–Pechora Province), in *Formatsii goryuchikh slantsev* (Oil Shale Formations), Baukov, S.S. and Kotlukov, V.A., Eds., Tallinn: Valgus, 1973, pp. 53–70.